12-2019

Standard Design for Nebraska County Bridges

Chungwook Sim

Jiong Hu

Maher K. Tadros

Alexander Bleyhl

David Gee

NEBRASKA
Good Life. Great Journey.
DEPARTMENT OF TRANSPORTATION

University of Nebraska Lincoln

Standard Design for Nebraska County Bridges

Final Report
M-064

Chungwook Sim, Ph.D.
Assistant Professor
Department of Civil and Environmental Engineering
University of Nebraska-Lincoln

Jiong Hu, Ph.D.
Associate Professor
Department of Civil and Environmental Engineering
University of Nebraska-Lincoln

Maher Tadros, Ph.D., P.E.
Professor Emeritus
Department of Civil and Environmental Engineering
University of Nebraska-Lincoln

Alexander T. Bleyhl
Graduate Research Assistant
Department of Civil and Environmental Engineering
University of Nebraska-Lincoln

David M. Gee
Graduate Research Assistant
Department of Civil and Environmental Engineering
University of Nebraska-Lincoln

Nebraska Department of Transportation

December 2019

FINAL REPORT

M064

STANDARD DESIGN FOR NEBRASKA COUNTY BRIDGES

Submitted By

Chungwook Sim, Ph.D.
Principal Investigator

Jiong Hu, Ph.D.
Co-Principal Investigator

Maher Tadros, Ph.D., P.E.
Co-Principal Investigator

Alexander T. Bleyhl
Graduate Research Assistant

and

David M. Gee
Graduate Research Assistant

at

University of Nebraska-Lincoln

Submitted to

Nebraska Department of Transportation

1500 Nebraska Highway 2

Lincoln, Nebraska 68502

Project Duration (7/1/2016 to 12/31/2018)

December 31, 2019

TECHNICAL REPORT DOCUMENTATION PAGE

1. Report No. SPR-1(17) M064	2. Government Accession No.	3. Recipient's Catalog No.
4. Title and Subtitle Standard Design for Nebraska County Bridges		5. Report Date December 31, 2019 6. Performing Organization Code:
7. Author(s) Chungwook Sim, Jiong Hu, Maher Tadros, Alexander Bleyhl, and David Gee		8. Performing Organization Report No.
9. Performing Organization Name and Address University of Nebraska-Lincoln, Department of Civil and Environmental Engineering, Peter Kiewit Institute, 1110 South 67th St., Omaha, NE 68022		10. Work Unit No. 11. Contract or Grant No.
12. Sponsoring Agency Name and Address Nebraska Department of Transportation (NDOT) 1500 Nebraska Highway 2 Lincoln, NE 68502		13. Type of Report and Period 14. Sponsoring Agency Code
15. Supplementary Notes		

16. Abstract

Many county-owned bridges in Nebraska need replacement due to their structural deficiency. Most of the bridges needing replacement are in the 40 to 60 ft range. This span range lacks a standard design that fits Nebraska county practices in terms of speed and simplicity of construction. The current systems being used are (a) Precast 1 by 2 ft planks which can span up to 30 ft, (b) Cast-in-place slab bridges which can span up to 50 ft but require extensive field formwork, concrete placing, and curing, and are best when constructed in three-span units, and (c) Inverted tees which can span 40 to 80 ft, but require cast-in-place decks. The objective of this research project is to develop and evaluate a cross section that can be easily configured for optimal structural efficiency across a range of spans from 40 to 60 feet, while reducing the number of shear keys, and retaining the ease of construction presented by the plank design. To achieve this objective, four phases of research were conducted. The first phase included evaluating various sections for spans up to 60 ft. This phase was completed through an extensive literature review and a, new type of cross-section was proposed in this study. The second phase of the research evaluated a new type of transverse connection to connect adjacent units of the proposed cross section for the proposed state county bridge system through small-scale testing on ten slab specimens. The third phase of the research includes testing

five sets of full-scale bridge specimens to evaluate the system behavior, including the performance of the proposed transverse connection that included the new type of mechanical connection, staggered rebar splice joints with a commercial high-performance concrete used for the shear key, and full-scale specimen with the staggered splice joint filled with three different types of high performance. Finally, the last phase of the research conducted a design review of various proposed sections and generated span charts that could be implemented for Nebraska County bridge design. Test results indicated that the new type of mechanical joint system (transverse connection of adjacent precast beam bridges) can resist an experimental joint moment of 38 ft-kip on average, provided that the maximum spacing between mechanical joints along the bridge span does not exceed 4 ft. It was also noted that the high-performance concrete can carry a joint moment of 17.5 kip-ft per foot length which is 2.5 times larger than the equivalent moment carried by the mechanical joint system with self-consolidating concrete grout. Other possible designs that were not tested through the small scale or full-scale experimental program were proposed by a local engineering firm in Omaha and reviewed in this research. The final standard design and design span charts are proposed for Nebraska County Bridges based on literature review, small scale testing, full-scale testing, and engineering calculations.

17. Key Words	18. Distribution Statement		
county bridges; longitudinal shear key; plank; transverse connection; ultra-high-performance concrete			
19. Security Classification (of this report) Unclassified	20. Security Classification (of this page) Unclassified	21. No. of Pages	22. Price

ACKNOWLEDGMENTS

This study was financially supported by the Nebraska Department of Transportation (NDOT). Their support is gratefully acknowledged. The technical support and valuable discussions provided by the Technical Advisory Committee (TAC) of this project and e.Construct, USA, LLC is appreciated. This study was conducted at the Large-Scale Structures Laboratory located in both Lincoln and Omaha of University of Nebraska.

DISCLAIMER

The contents of this report are based upon work supported by the Federal Highway Administration under SPR-1(17) M064. Any opinions, findings, conclusions, or recommendations expressed in this publication are those of the author(s) and do not necessarily reflect the views of the Federal Highway Administration.

ABSTRACT

Many county-owned bridges in Nebraska need replacement due to their structural deficiency. Most of the bridges needing replacement are in the 40 to 60 ft range. This span range lacks a standard design that fits Nebraska county practices in terms of speed and simplicity of construction. The current systems being used are (a) Precast 1 by 2 ft planks which can span up to 30 ft, (b) Cast-in-place slab bridges which can span up to 50 ft but require extensive field formwork, concrete placing, and curing, and are best when constructed in three-span units, and (c) Inverted tees which can span 40 to 80 ft, but require cast-in-place decks.

The objective of this research project is to develop and evaluate a cross section that can be easily configured for optimal structural efficiency across a range of spans from 40 to 60 feet, while reducing the number of shear keys, and retaining the ease of construction presented by the plank design. To achieve this objective, four phases of research were conducted. The first phase included evaluating various sections for spans up to 60 ft. This phase was completed through an extensive literature review and a, new type of cross-section was proposed in this study. The second phase of the research evaluated a new type of transverse connection to connect adjacent units of the proposed cross section for the proposed state county bridge system through small-scale testing on ten slab specimens. The third phase of the research includes testing five sets of full-scale bridge specimens to evaluate the system behavior, including the performance of the proposed transverse connection that included the new type of mechanical connection, staggered rebar splice joints with a commercial high-performance concrete used for the shear key, and full-scale specimen with the staggered splice joint filled with three different types of high performance. Finally, the last phase

of the research conducted a design review of various proposed sections and generated span charts that could be implemented for Nebraska County bridge design.

Test results indicated that the new type of mechanical joint system (transverse connection of adjacent precast beam bridges) can resist an experimental joint moment of 38 ft-kip on average, provided that the maximum spacing between mechanical joints along the bridge span does not exceed 4 ft. It was also noted that the high-performance concrete can carry a joint moment of 17.5 kip-ft per foot length which is 2.5 times larger than the equivalent moment carried by the mechanical joint system with self-consolidating concrete grout. Other possible designs that were not tested through the small scale or full-scale experimental program were proposed by a local engineering firm in Omaha and reviewed in this research. The final standard design and design span charts are proposed for Nebraska County Bridges based on literature review, small scale testing, full-scale testing, and engineering calculations.

CHAPTER 1. INTRODUCTION

1.1 Background

Across the country many states are faced with the same issue of an aging infrastructure, and Nebraska is no different. Approximately, 60% of the bridges in the local system were constructed between the 1930's and 1960's. Of the 11,763-local system (county) bridges, 2,373 have been deemed structurally deficient (*http://www.nebraskalegislature.gov/pdf/reports/committee/transport/2014_lr528.pdf*). These statistics make Nebraska the 7th worst state for structural deficiencies in their rural bridge systems (approximately 1 in 5 rural bridges). Approximately 40% of the bridges built between 1930 and 1960 span between 40 to 60 ft, which is the primary focus of this project. This span range appears to be lacking a standard design that fits Nebraska county practices in terms of speed and simplicity of construction. The Nebraska Department of Transportation is working towards creating standard bridge designs that are easily constructed anywhere in the state, durable, and cost effective to replace these aging bridges.

The Nebraska counties currently use a relatively shallow plank cross section that is 2'-10" wide and 1'-8" deep (Figure 1.1) that can span between 30 to 40 feet. This cross section was selected many years ago due to it being within the weight constraints of the cranes that were owned by many of the counties at the time. For example, every county had a Bantom crane and the planks shown in Figure 1.1 were the largest size these cranes could pick up at that time.

These planks could also be easily cast anywhere in the state as shown in Figure 1.2 without a prestressing bed. These planks are connected transversely with a shallow shear key and welded together at the top of the planks (Figure 1.2). Although the planks have proven to be a viable option over the years there are still some limitations. It currently takes 14 to 16 of these

planks to construct a typical country bridge with the necessary width (30 – 32 ft wide) which creates a large number of longitudinal shear keys (Figure 1.3).

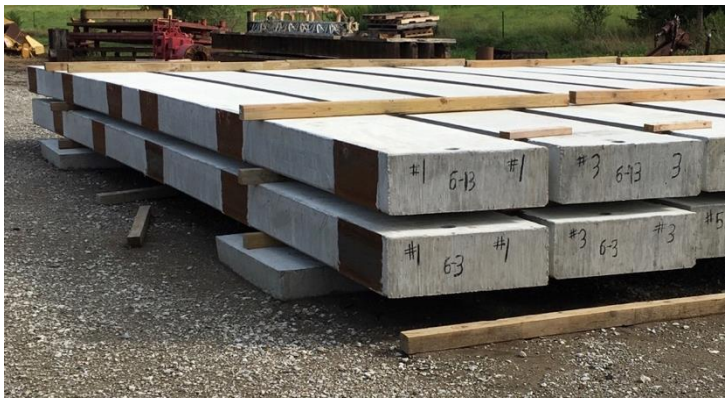

(a) (a) Planks used in multi-beam bridges in Nebraska

(b) (b) Reinforcing steel cages

Figure 1.1: Typical Non-prestressed Precast Planks used for Nebraska County Bridges (photos taken at the Midwest Underground casting facility)

(a) Simple steel forms to cast planks (photo taken at the Midwest Underground Casting Facility in Nebraska)

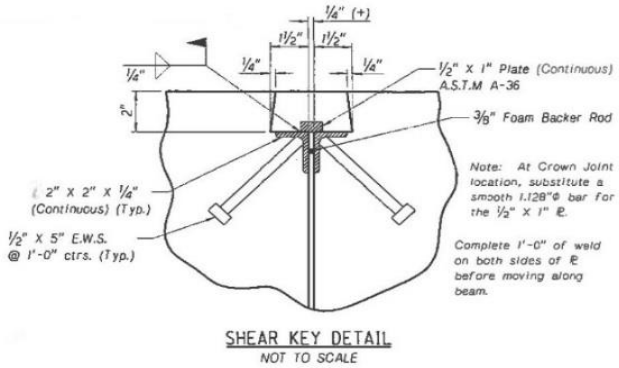

(b) Shear key details for the joint connections

Figure 1.2: Steel Casting Forms and Shear Key Details for the Planks

The grout between these longitudinal shear keys easily cracks and creates a path for water and chlorides to penetrate through. Even though deicing salt may not be used in the counties, vehicles that cross the bridges can bring chlorides into these joints. The structural performance

of these pieces is governed by their shear key. In addition, some of these shear keys are connected with a continuous weld which creates a tedious task in construction and in some cases can create additional camber to the planks.

Figure 1.3: Grouts Between Longitudinal Shear Keys

1.2 Research Objective

The objective of this research project is to develop and evaluate a standard cross section that can be modified to be used for spans up to 40 to 60 feet, while reducing the number of longitudinal shear keys, and retaining the ease of construction offered by the plank design. In addition to the proposed section, different types of transverse connections will be evaluated through an experimental program.

1.3 Research Scope

This research was conducted in three phases such that a comprehensive design standard can be developed and implemented. The first phase evaluated various bridges sections up to 60

ft. This included solid planks, voided planks, box beams, and stemmed members. At the end of this phase, a preferred standard section was chosen. The second phase was composed of an experimental program that includes a small-scale testing of these longitudinal shear key connections and their joint capacity of the most promising section for Nebraska. This phase included the development of a new connection joint detail. The third phase included a full-scale testing of the proposed section with different types of transverse connections. The results of the three phases are integrated with design reviews conducted by a local engineering firm in Omaha to provide a final design for a simple, structurally efficient, and economical bridge option for bridges with 40 to 60 ft span length. The results of this research from the three phases will be integrated into developing design and construction recommendations for Nebraska Department of Transportation that can systematically be used for replacing aging Nebraska County Bridges.

CHAPTER 2. LITERATURE REVIEW

2.1 Introduction

Many of the Nebraska county bridges needing replacement are in the 30 to 60 ft range. This span range appears to be lacking a standard design that fits Nebraska county practices in terms of speed and simplicity of construction. The current systems being used are 1) precast one by two feet planks introduced in Chapter 1 which can span up to 30 ft (heavily used in Nebraska counties), 2) cast-in-place slab bridges which can span up to 50 ft but require extensive field formwork, concrete placing, curing, and are best when constructed in three-span units, and 3) inverted tees which can span between 40 to 80 ft, but require cast-in-place decks. This chapter provides a literature review regarding cross sections (including solid planks, void planks, box beams, and stemmed members) that can span up to 60 ft and are adjacent to each other (butted up against each other). Previous research that includes computational analysis, experimental testing, field monitoring, or synthesis studies of the cross sections mentioned above are provided in this chapter.

2.2 Computational Analysis

2.2.1 University of Illinois Study (1965)

The experimental and numerical studies conducted by Newmark and Siess (1942) provided the guidelines for the load distribution factors that were introduced in the earlier AASHTO Standard Specifications for Highway Bridges (1957) which was a study of simple-span I-Beam bridges. Based on these earlier studies conducted at the University of Illinois, Pool et al. (1965) evaluated multibeam bridges (Figure 2.1) and suggested a method of calculating joint forces in the longitudinal shear keys through numerical studies.

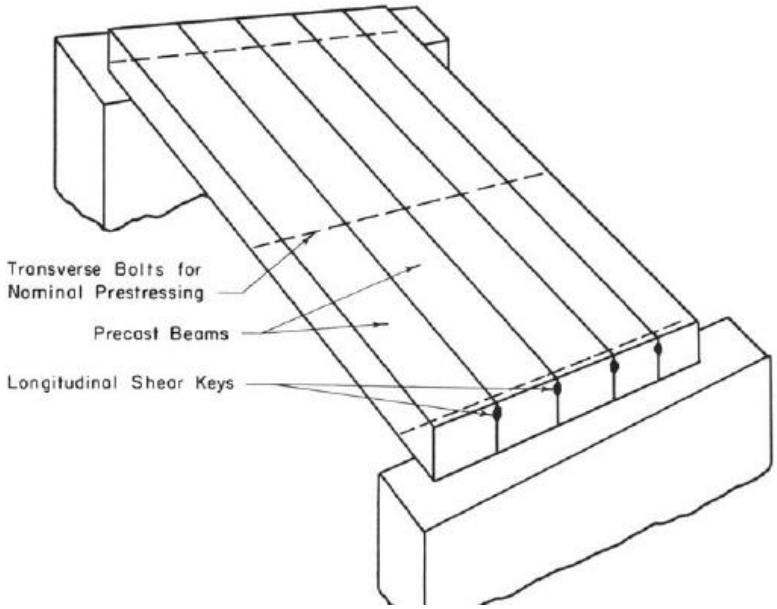

Figure 2.1: Multibeam Bridge with Longitudinal Shear Keys (figure retrieved from Pool et al. 1965)

Five multibeam bridges with four or eight elements were used in the parametric studies of this research. The authors assumed that the longitudinal shear keys that are used to connect these individual elements are a continuous hinge that transmits longitudinal, lateral, and vertical force at the joint and has no relative displacements. A number of tables that consisted of the longitudinal, lateral, and vertical joint forces for a concentrated wheel load applied at specific locations were reported. The tabulated results can be applied to similar types of structures and multi-beam bridges that are solid planks, hollow sections, or box cross sections. The conclusions of this study found that there are discontinuities in the longitudinal joint forces where the concentrated wheel load was applied. Lateral and vertical joint forces were distributed along the joint as the wheel loads passed over the bridge. However, high concentrated forces will not be observed in an actual bridge as shown in this study if lateral post-tensioning is present. This research at the end concludes that the limitations of the study can be corrected through further experimental research on shear keys to adequately model the joint behavior.

2.2.2 Texas A&M Study (1999, 2001)

The research team at the Texas A&M University looked into the lateral distribution factors of multi-beam prestressed concrete box girders with a composite concrete deck slab for twenty-two Texas Department of Transportation bridge configurations. The springs that were implemented in these models at the grouted joints for parametric studies considered the longitudinal, lateral, vertical, and rotational stiffness in the transverse direction (Figure 2.2).

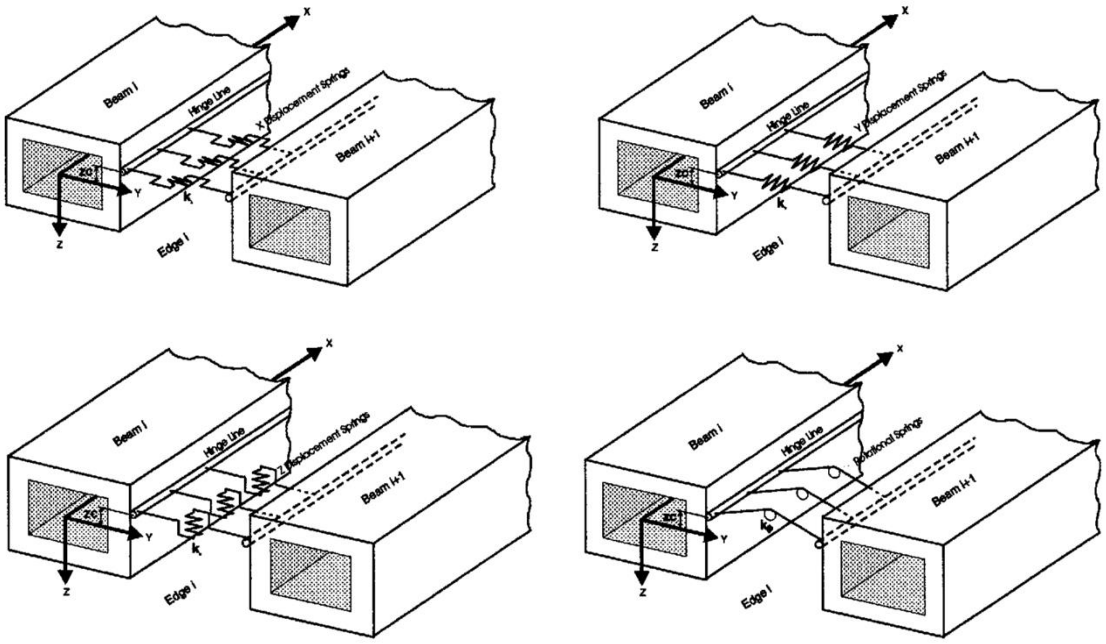

Figure 2.2: Four Spring Models connecting Adjacent Beams (retrieved from Jones, 1999)

This research team conducted further studies on the lateral connection of double tee bridges and looked into various keyway details for multi-beam bridges. As a result of this study, Jones (2001) proposed a new connection detail (Figure 2.3) for these types of bridges and evaluated the new connection behavior through static and cyclic testing.

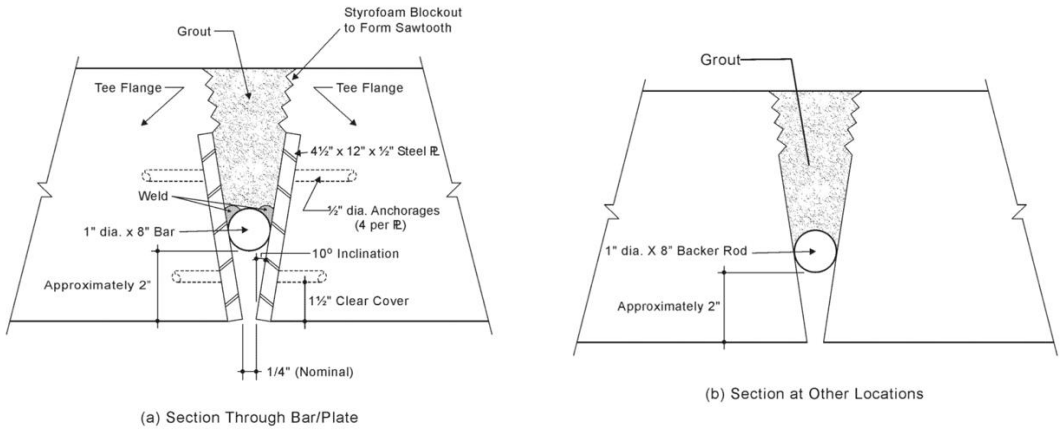

Figure 2.3: New Types of Keyway Details introduced in Texas Study for Double Tee Multibeam Bridges (retrieved from Jones, 2001)

2.2.3 University of Nebraska Study (2011)

In this study, Hanna et al. (2011) suggested a different approach on how adjacent box beam bridges should be designed without having post-tensioned transverse connections. Instead of post-tensioning the adjacent girders, the research team looked into two different joint systems that eliminate the need for post-tensioning, diaphragms at the end and intermediate supports, and a cast-in-place concrete topping. Both connection types (the wide-joint or narrow-joint shown in Figure 2.4) utilized the AASHTO PCI box section. The wide-joint system connected the top and bottom flange by a ¼ in. confinement spiral around high tensile coil rods with an extra cavity formed out to allow development length to take place. To reduce the cost of the wide-joint system, the research team recommended using self-consolidating concrete in the shear keys to reduce the time and cost associated with grouting. The narrow-joint system utilized a ¾ in. diameter threaded rod at every eight feet with a 5 in. long coupling nut to connect the two pieces at the top and bottom.

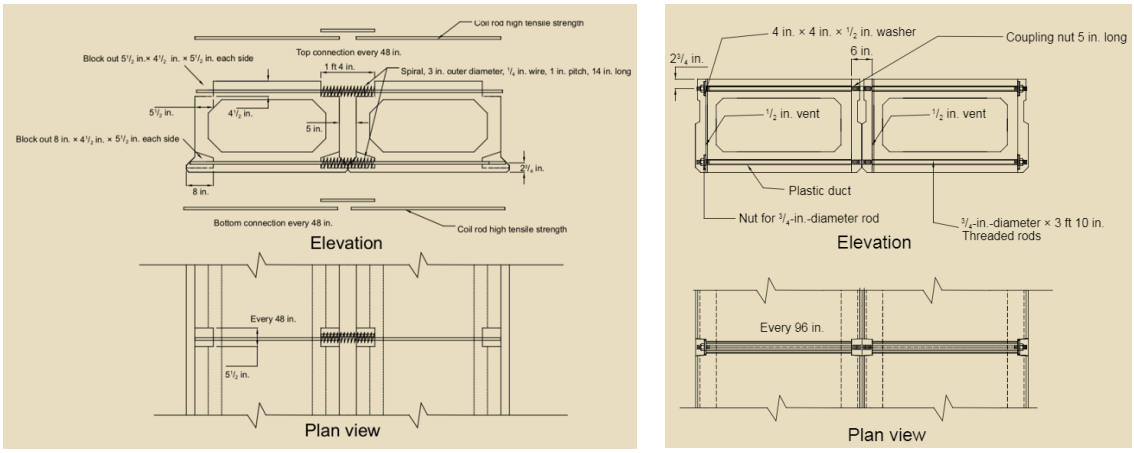

Figure 2.4: Wide-joint and Narrow-joint Connection Details introduced in Nebraska Study (retrieved from Hanna et al., 2011)

Both of these joints were modeled as shell and frame elements to develop design charts before testing an actual specimen. These design charts displayed the required tension force in the connection for various bridge widths, and span-to-depth ratios. Based on these parametric studies, the research team built three specimens to verify their design charts. An IDOT connection using diaphragms and a single mid-level transverse tie, the narrow-joint connection, and the wide-joint connection made up the three specimens to be tested. All three connections were tested both under static and fatigue load conditions. The moment capacity of the IDOT system with a 5 in. non-composite concrete topping was 179 kip-ft while the wide-joint system achieved a capacity of 126 kip-ft. The narrow-joint system achieved a moment capacity of 119 kip-ft. The research team compared these test results to their finite element models and found a difference of 19%, 0.8%, and a 30.3% between the theoretical capacity and the actual tested capacity for IDOT connection, wide-joint connection, and narrow-joint connection, respectively. With this data the research team concluded that the connections could be designed to achieve comparable results without diaphragms or post-tensioning, which would be an economical and practical alternative.

2.3 Experimental Testing, Field Monitoring, and Forensics

2.3.1 University of Washington Study (1986)

This research conducted at the University of Washington was another milestone study that newly included the load distribution factors for precast multi-beam bridges which was not introduced in the earlier 1983 AASHTO Standard Specifications for Highway Bridges that was based on the studies completed in University of Illinois. Stanton and Mattock (1986) found through their parametric grillage analysis that the span-to-width ratio and the ratio of flexural-to-torsional stiffness are the most important factors in load distribution in these multi-beam systems and the results of their study will apply to multi-beam bridges with any cross section. The authors stated that unless the bridge is very short and wide, the load distribution factor introduced in this study can be applied to various single-stem and multi-stemmed precast bridge sections. The live load distribution per lane for moment in interior beams tabulated in Table 4.6.2.2.b-1 in the current AASHTO LRFD Bridge Design Specifications (2010) is based on the results of this study.

This research also looked into the details of the connections in precast multi-beam bridges. The authors conducted a nationwide survey that was collected through state and county bridge engineers and precast producers who provided details for the different shear keys they used (Figure 2.5).

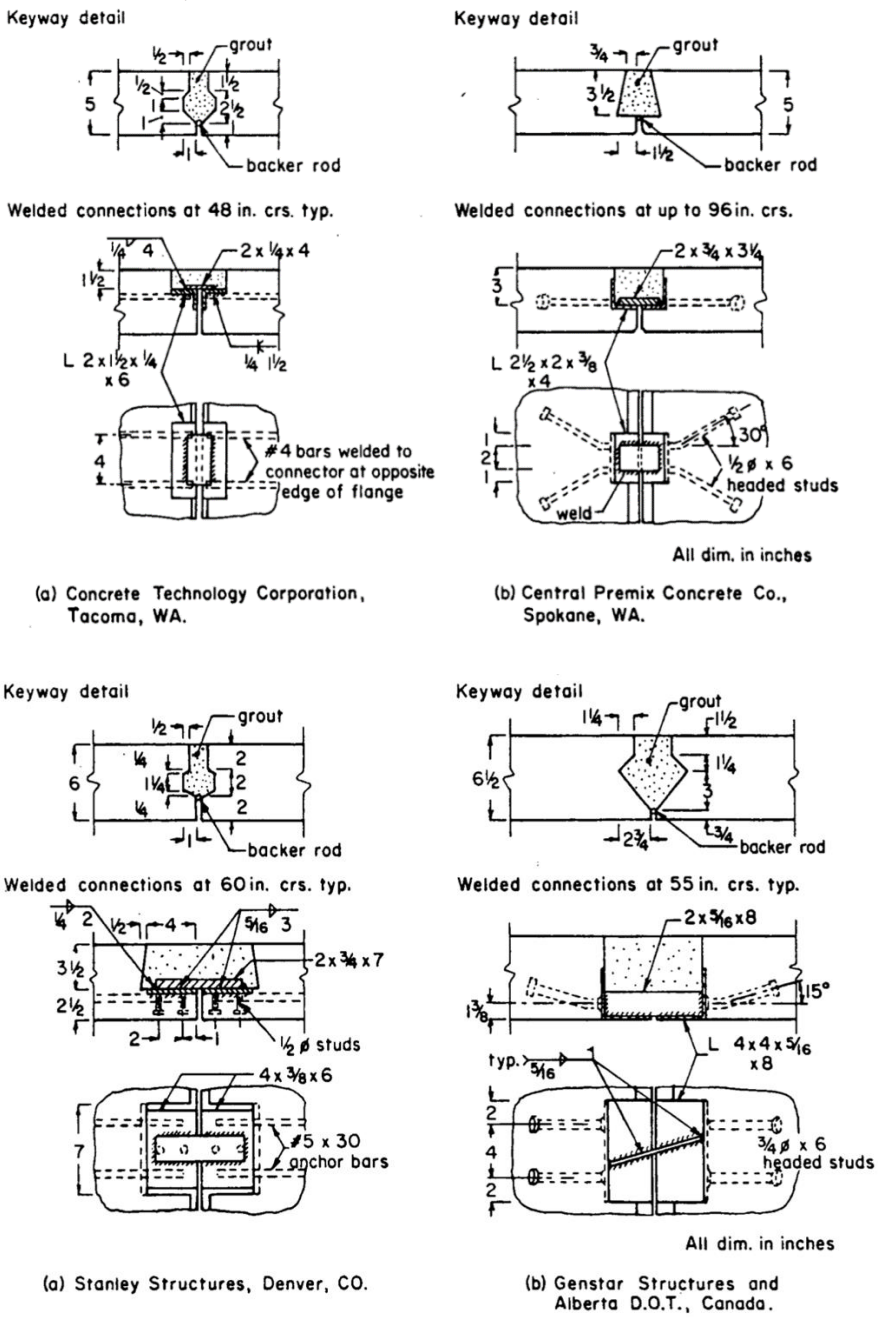

Figure 2.5: Examples of Shear Keyway Details (retrieved from Stanton and Mattock, 1986)

The survey showed that standard design and details were lacking in these connections and that most of the joints were designed based on previous experience or so called “rules of thumb”. As a result, Stanton and Mattock (1986) evaluated the shear strength of a typical type of joint (grouted shear keys and welded connectors) through experimental testing and suggested a

shape for grout keys (Figure 2.6). The authors did recommend that further research should be conducted to verify the local joint forces in grouted joints caused by wheel loads.

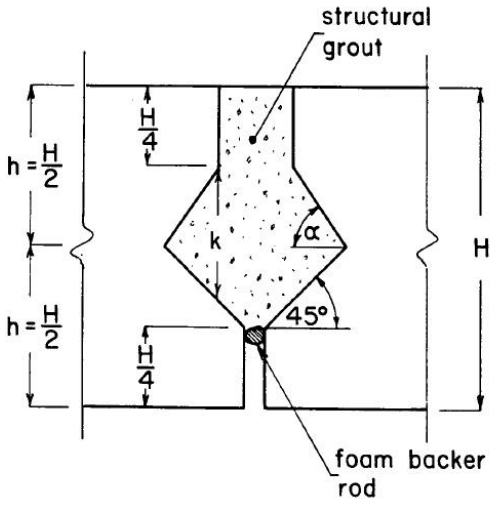

Figure 2.6: Recommended Shape of Grout Key from University of Washington Study (retrieved from Stanton and Mattock, 1986)

2.3.2 Case Western University Study (1995)

A series of field tests were conducted by researchers (Huckelbridge et al., 1995) at the Case Western Reserve University to evaluate the shear key performance of adjacent multibeam box girder bridges in Ohio. The typical grouted shear keys at the longitudinal joints between adjacent girders are shown in Figure 2.7. The relative displacement between the girders across joints were measured through multiple passes by a pre-weighted, tandem-axle dump truck. All six bridges that were monitored throughout this process showed differential displacement across joints indicating fractures in the grouted keys. It is interesting to note that this research also identified that the typical tie bars that were used by the Ohio Department of Transportation at the time of research (1 in. diameter mild steel tie bar at distances up to 25 ft) at the girder mid-height in transverse diaphragms had little effect and still should signs of shear key failure and relative

deflection between girders. The research team recommended moving the shear key to neutral axis of the box girder section.

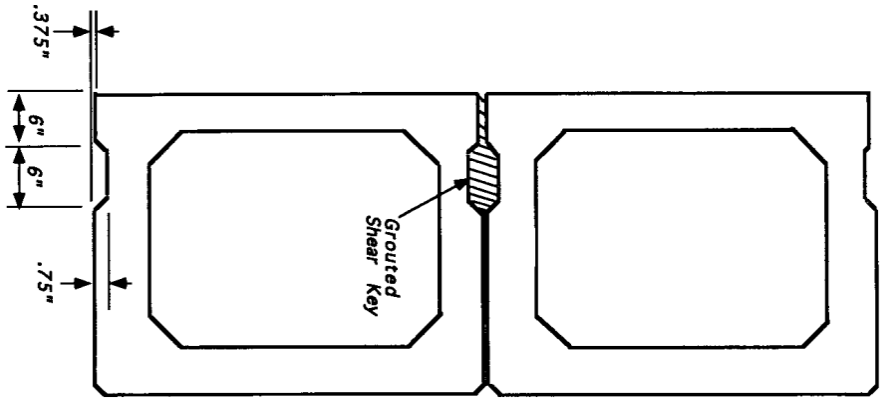

Figure 2.7: Grouted Shear Keyway Detail for Adjacent Box Girders (retrieved from Huckelbridge et. al., 1995)

2.3.3 University of Cincinnati Study (1998)

Full-scale testing on adjacent box girder bridges were conducted by Miller et al. (1998) at the University of Cincinnati to evaluate the grouted shear keys under temperature and cyclic loads. The variables selected for the full-scale testing includes 1) a non-shrink grout at the top keyway, 2) an epoxy grout at the top keyway, and 3) non-shrink grout with the keyway located near the neutral axis of the girder (lowered keyway – see Figure 2.8). One of the keyways were grouted in late fall while the other two keyways were constructed during summer. All of the cracks initially found in the keyway were initiated through large changes in strain due to temperature change. Based on the fatigue test with HS20-44 truck wheel load, it was observed that no additional cracks initiated due to the cyclic loads other than the crack formed due to thermal loads. However, the cracks formed through temperature changes did propagate further into the section due to the truck load. The specimen with a non-shrink grout keyway that was

placed at the top of the girder was subjected to 41,000 cycles while the other two specimens were loaded up to 1,000,000 cycles. It was observed that epoxy grout did work well but the difference in coefficient of thermal expansion with concrete could cause high stresses in the keyways and this research team believed more studies would be required with epoxy grouts. Although, some cracks were still found, this research study concluded that the neutral axis keyway performs better than top keyways and recommended that the keyways in most of the partial-depth joints should be moved down to the neutral axis of the girder.

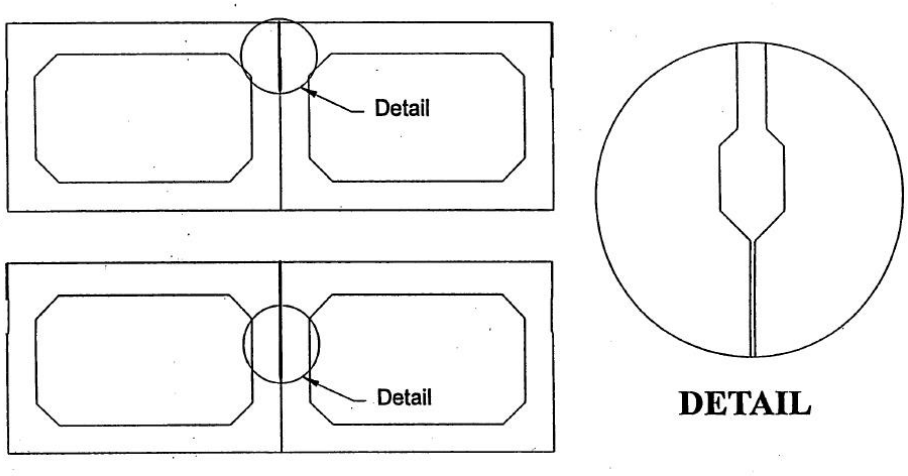

Figure 2.8: Top and Suggested Lower Keyway (retrieved from Miller et. al., 1998)

2.3.4 Lehigh Study (2010)

In 2007, the state of Pennsylvania had 3,291 adjacent prestressed box beam bridges in service and of those 590 were labeled as structurally deficient. On December 27th, 2005 a fascia beam of the Lake View Drive Bridge in Pennsylvania failed under service loading (Figure 2.9). Although these incidents are never welcomed, it did allow a team of researchers (Naito et al., 2010) to investigate what caused this bridge to fail. This bridge was inspected by the state in 2004.

Figure 2.9: Forensic Examination of Non-composite Adjacent Precast Prestressed Concrete Box Beam Bridge Failure in Pennsylvania (retrieved from Naito et al., 2010)

From this inspection it was noted that an impact may have happened to a specific beam, and that 20 of the 60 strands were broken in that member. The other members were only moderately damaged and the bridge was rated as poor (four on a scale of zero to nine). Beam replacement was labeled as a priority. It was later discovered after the collapse through inspection that 39 of the 60 strands were severely damaged through corrosion and it was believed that there was no indication of an impact before the collapse. This bridge had four spans each of which had eight pretensioned box beams with an approximate two-inch bituminous overlay with no water-proofing membrane. The bridge beams were poured and erected in 1960. The clear cover from the strands to the exterior surface for the beam that collapsed ranged from 1 foot and 5/16 inches to 1 foot and 9/16 inches which met the 1953 AASHTO Standard Specifications for

Highway Bridges but had less than the minimum cover of 1.5 inches specified by the 1965 AASHTO specifications.

The next item the research team investigated was the shear reinforcement. The shear stirrups were not placed below the bottom layer of prestressing strands and for the ease of construction an L-shape was used and placed between the first and second layer of strands which was common practice at the time the bridge was constructed. It should be noted this is no longer a standard practice. It was also found that many of the top and bottom L-shaped stirrups were not physically lap-spliced in the middle and were separate from each other. Due to this lack of splice contact and also the short development length provided (12 in.), the authors were concerned about the shear capacity for these box girders. An interesting note for this bridge was the way in which the void was formed and the drains that were used. The voids were constructed with the use of cardboard void forms. It was found that these forms moved during concrete placement and created a final product that did not match the design drawings with regards to wall thickness. In the late 1950's, ¾ inch diameter drains were placed in both the top and bottom flange. These drains allowed moisture to enter the void and wet the cardboard. This cardboard eventually degraded and possibly blocked the exit drains leading to excess water being held inside the void. The excess water not only added to the potential corrosion of strands but also increased the total live load on the member. Both air content and concrete strength were found to be within the design requirements. Upon investigation it was found that over 40% of the strands were found to be in serious or critical condition, which means that the strands were deteriorated to a point that seriously affected the primary structural components of the bridge and corrective action was needed based on the PennDOT Superstructure Condition Rating Guidelines. With all the forensics of this bridge, there were two major takeaways with respect to

bridge inspection and evaluation that the research team suggested to prevent a similar failure. The first was to deduct 125% of the total cross-sectional area from all exposed strands when calculating the structural capacity. The other suggestion based on the observations of this collapse case was that strands adjacent to or intersecting a crack should not be considered as an effective strand due to possible corrosion.

2.4 Synthesis Study

2.4.1 University of Nebraska Study (1996)

Researchers at the University of Nebraska (El-Remaily et al., 1996) took an in-depth look into the transverse design details of adjacent precast prestressed concrete box girder bridges in the United States and in Japan. Their research began looking into current practices here in the United States and associated problems with the current practice that have been recorded during bridge inspections. The surveys showed it was commonly noted that there was longitudinal cracking along the grouted shear keys with reflective cracking in the overlay above the shear keys. These cracks often lead to penetration of water and chemicals that later creates spalling, staining, and reinforcement corrosion. When reviewing the common practice in Japan it was noted that the box girders were very similar in design, except for the shape and size of the shear keys which were much larger than the ones in the US. In addition, higher levels of transverse post tensioning were used in Japan compared to the practice in the US. This practice in Japan led to longitudinal cracking to be seldom reported. After comparing the practices in both countries, El-Remaily et al. (1996) proposed a modification to the common practice in the United States. A design chart consisting of the required effective prestressing force at the diaphragm in the midspan for various bridge widths for four standard AASHTO-PCI box girders (depth of 27, 33, 39, and 42 in.) were provided in this study. The study states that the required post-tensioning

force for the quarter-point diaphragms are found to be similar with the force required in the midspan. For the end diaphragms, the study suggests to provide a minimum of 250 psi for effective post-tensioning stress. All of these post-tensioning forces are recommended to be applied through tendons at both the top and bottom in order to provide sufficient flexural strength. Based on the recorded history of Japanese bridges the researchers believe this would be an economical solution to increase the longevity of adjacent precast prestressed concrete box girder bridges in the United States.

2.4.2 University of Nebraska Study (2009)

Hanna et al. (2009) looked into the design practice of transverse post-tensioning of precast, prestressed adjacent-box-girder bridges (Figure 2.8) and provided an extensive literature review. Based on their literature review, they stated that the current design practice of box girder bridges without post-tensioning often leads a recurring problem of longitudinal cracking along the grouted joints. They introduced a bridge failure that took place in Pennsylvania on December 27, 2005 and in a railroad bridge in Nebraska in 2007 that had a similar design. Hanna et al. (2009) also introduced numerous practices across the United States, Canada, Japan, and Korea including composite or non-composite systems, full-depth or partial-depth shear keys, and designs with or without the presence of post-tensioning.

The team noted a particular study that looked into practices in the state of New York (Lall et al., 1998). After 1992, the state of New York changed their design standards for precast concrete girders 1) to have full-depth shear keys, which was only about 12 in. from the top previously, and 2) to increase the number of transverse tendons to three for short span bridges less than 50 ft which had no transverse tendons prior to 1992. Lall et al. (1998) reported that

after the standards were implemented only 23% of these types of bridges built within the three-year span after the change showed longitudinal cracking in the joints.

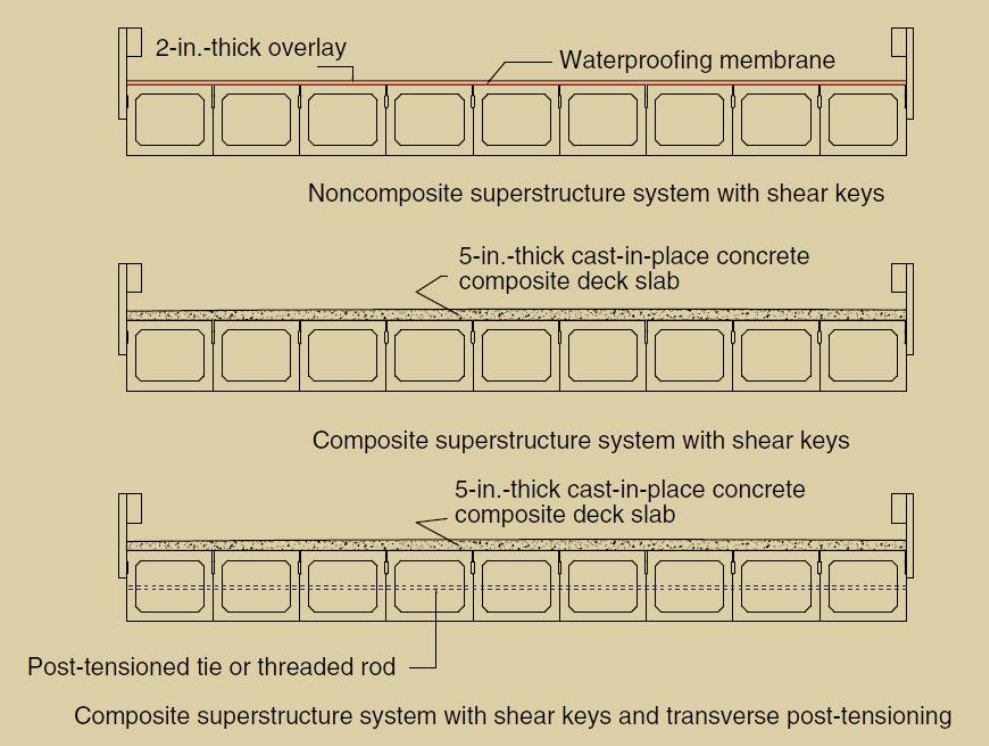

Figure 2.10: Various Practices in Adjacent Box Girder Bridge Design and Details (retrieved from Hanna et al., 2009)

Another study (Greuel et al., 2000) introduced a high performance concrete adjacent box girder bridge built by the Ohio DOT which consisted of a shear key at the mid-depth of the section. These girders were transversely tightened with threaded rods at the ends and quarter points of the bridge. The bridge was loaded with four DOT trucks and the girders were observed to be working together based on the smooth deflection curve the girders created. Lall et al. (1998) also listed the recommendations and input provided from the PCI subcommittee survey conducted through the 29 states and 3 provinces in United States and Canada regarding the lessons learned from the design and construction of adjacent box girder bridges. A few preventive actions that can be taken to reduce or eliminate the cracks that were reported from

many transportation agencies that participated in the survey. These suggestions included 1) having a cast-in-place concrete deck on top of the adjacent girders, 2) using non-shrink grout, 3) using full-depth shear keys rather than partial-depth keys, 3) applying transverse post-tensioning that helps with load distribution, minimizes differential deflections, and minimizes longitudinal cracking, 4) having intermediate and end diaphragms to provide necessary stiffness in the transverse direction, 5) including wide bearing pads and seats to eliminate rocking while grouting the joints, and 6) eliminating the use of welded connections between adjacent girders that cause inadequate sealing of joints.

Based on the extensive literature review, Hanna et al. (2009) emphasized the needs in studying the amount of post-tensioning needed to limit the differential deflection between girders. They finalized the study by conducting a parametric study using grid analysis to find the required amount of effective post-tensioning force for different bridge widths, depths, span lengths, and skew angles. They provided a simplified formula that gives a conservative estimate of the required transverse post-tensioning force for various conditions and also provided a useful design example for a single span bridge as a summary.

2.4.3 Russell (2011)

This research provides a summary of design, construction, maintenance, and inspection practices for adjacent precast concrete box beam bridges. From a nationwide survey conducted through a NCHRP Synthesis 393 (Russell 2009) study, it was reported that approximately two-thirds of the state departments of transportation use adjacent box beam bridges. The two major problems identified were longitudinal crack along the joint and water and chloride penetration through the joint (Figure 2.11). Most of the state departments of transportation reported that sufficient transverse post-tensioning and the use of concrete topping slab would be the most

effective way to increase the long-term performance. In addition, most of the longitudinal keyways between these adjacent beams were reported to be partial depth and it would be beneficial to require full-depth shear keys in design to increase the long-term performance of these structures.

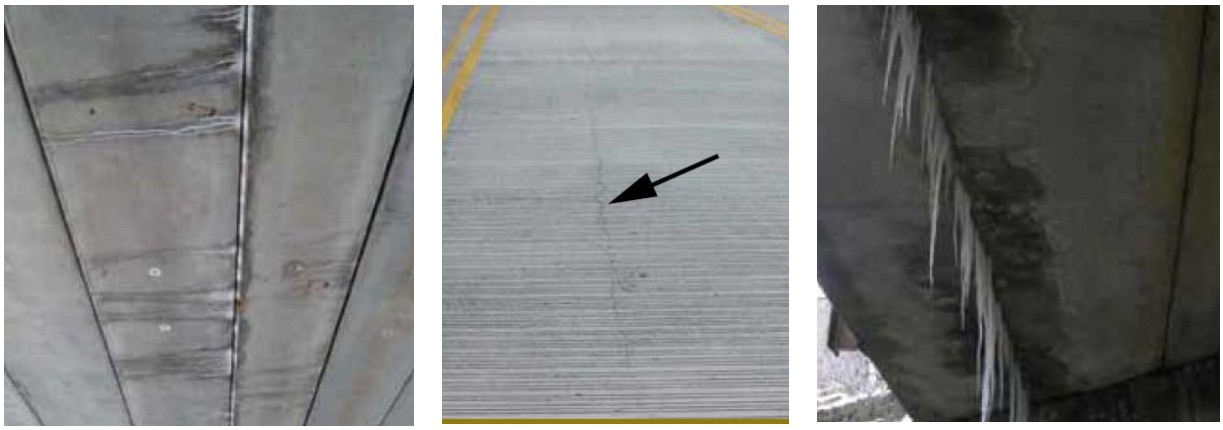

Figure 2.11: Major Problems reported in Adjacent Beam Bridges: Longitudinal Crack along the Joint and Water and Chloride Penetration (retrieved from Russell, 2011)

2.5 Summary

Based on the literature review that includes computational analysis, experimental testing, field monitoring, and synthesis studies on bridges with adjacent beams it is obvious that the lateral load distribution and load transfer between individual beams are highly dependent on the keyway joint details. Although, many different types of shear keyway details were developed from the nationwide surveys and field measurements, it was identified that these grouted joints still crack, create longitudinal cracks on top of the bridge deck, and create a path for water or chloride leakage. Many of the state and county engineer, and precast producers identified that the solutions to this recurring problem could be 1) providing a full-depth shear key, 2) post-tensioning the adjacent beams in transverse direction, or 3) topping these adjacent beams with cast-in-place deck. The objective of this research is to suggest a standard design that can span up

to 40 to 60 feet (high needs in Nebraska counties) while retaining the ease of construction factor presented by the plank design. In order to resolve the problems seen in this literature survey without complicating the construction for counties (not introducing post-tensioning, or including cast-in-place decks), this study is suggesting a "flexible" precast cross section (Figure 2.12), which is 8 ft wide and depending on the span length varies the depth to be between 1 to 3 ft. This cross section includes the deck which reduces the cast-in-place construction and is wider than a typical single tee section. The width of the web is wider than the typical single tee cross section but is shallower than a typical bulb tee and is stable enough to stand alone. With an 8 ft wide cross section, that is not very different than a wider plank with a stem in the middle, this section will create smaller number of joints for a typical county bridge that has a width of 25-35 ft. The total weight for these cross sections would be 13, 22, and 40 tons for a span length of 30, 40, and 60 ft span length, respectively. This would allow Type I, II, and III cross sections shown in Figure 2.12 to be handled easily using the county level cranes. Concrete diaphragms can be added at the ends to increase the stability at supports. This study will conduct small-scale and full-scale testing on various types of joint details for this cross section and also investigate the possibilities of implementing high-strength steel reinforcement as main reinforcement.

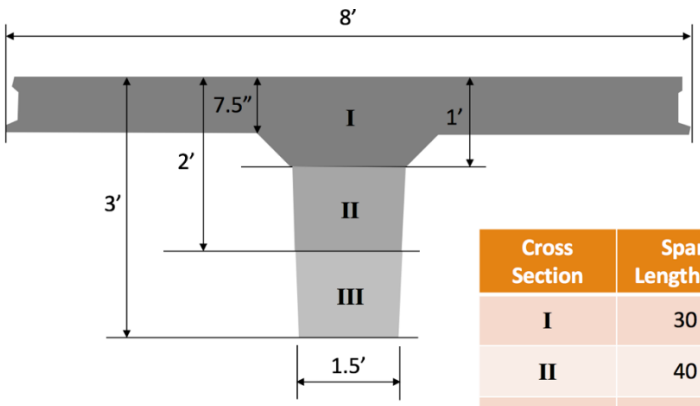

Cross Section	Span Length (ft)	Weight (US ton)
I	30	13
II	40	22
III	60	40

Figure 2.12: Proposed Standardized "Flexible" Cross Section for Nebraska County Bridges

CHAPTER 3. MECHANICAL CONNECTION TEST PROGRAM

3.1 Introduction

The objective of this phase of the research is to investigate the shear and moment capacity of a new type of mechanical connection that is proposed to be used in connecting adjacent precast bridge sections proposed in the previous chapter. Each mechanical joint consists of four all threads (coarse or fine threaded) with nuts, an alignment plate, an anchor plate, and a 1.25 in. ASTM A490 bolt with nut to connect the two slabs as shown in Figure 3.1. Three and four-point bending tests were conducted to evaluate the shear and moment capacity of the proposed mechanical connection for the adjacent bridge sections.

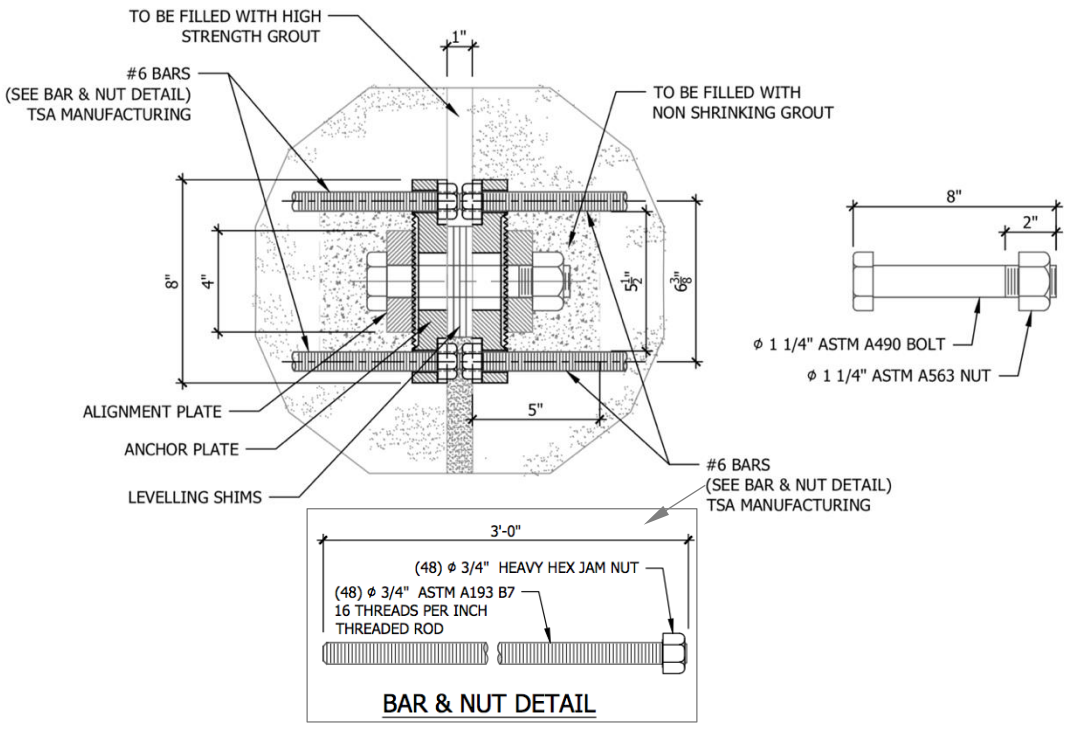

Figure 3.1: Mechanical Connection Details for Precast Adjacent Beam Bridges

3.2 Slab Specimen Design and Variables

Each slab was built to be 3 ft-11.5 in. by 4 ft having the grouted keyway in the middle of the slab. After grouting the 1 in. gap left between the slabs the connected slab specimen becomes 8 ft by 4 ft. This is to represent a cut section of half of the precast beam connected with half of the other adjacent beam, simulating having transverse connections every 4 ft for the 8 ft wide precast section. Each slab was reinforced with top and bottom mat of #4 bars as shown in Figure 3.2. The slab specimens are 7.5 in. deep which is the depth of the proposed section (Figure 2.12) including the deck.

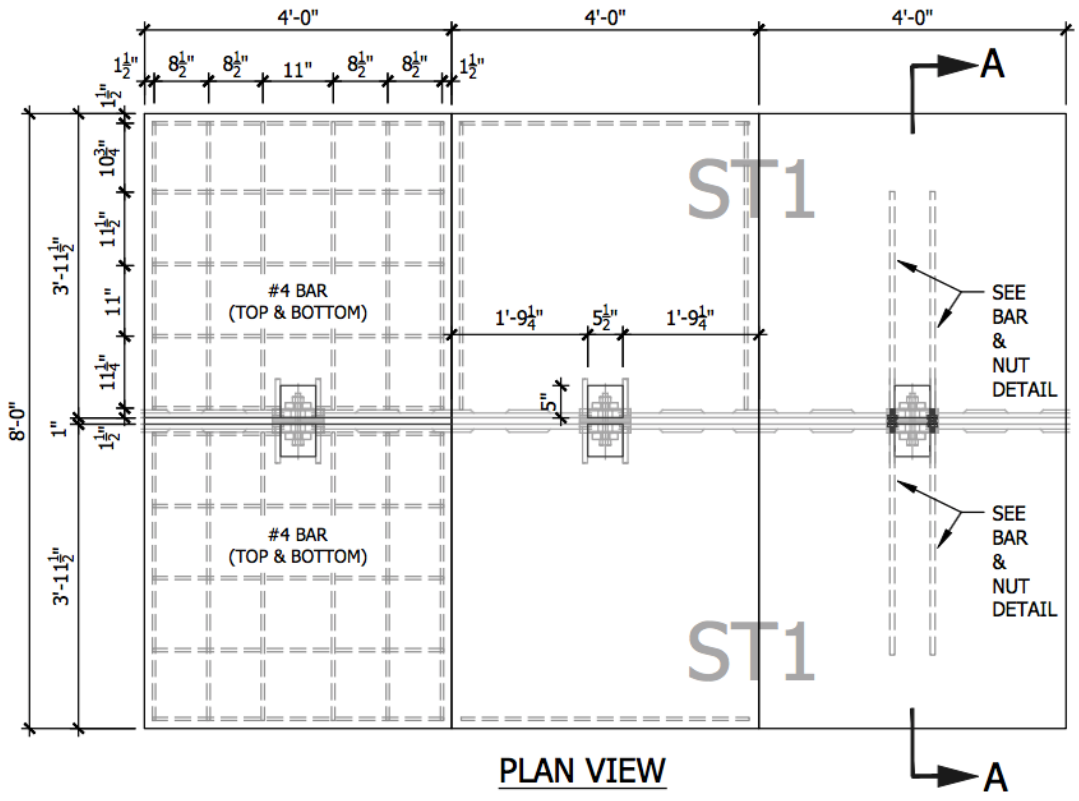

(a) rebar layout (b) bolt connection (c) threaded bar connection

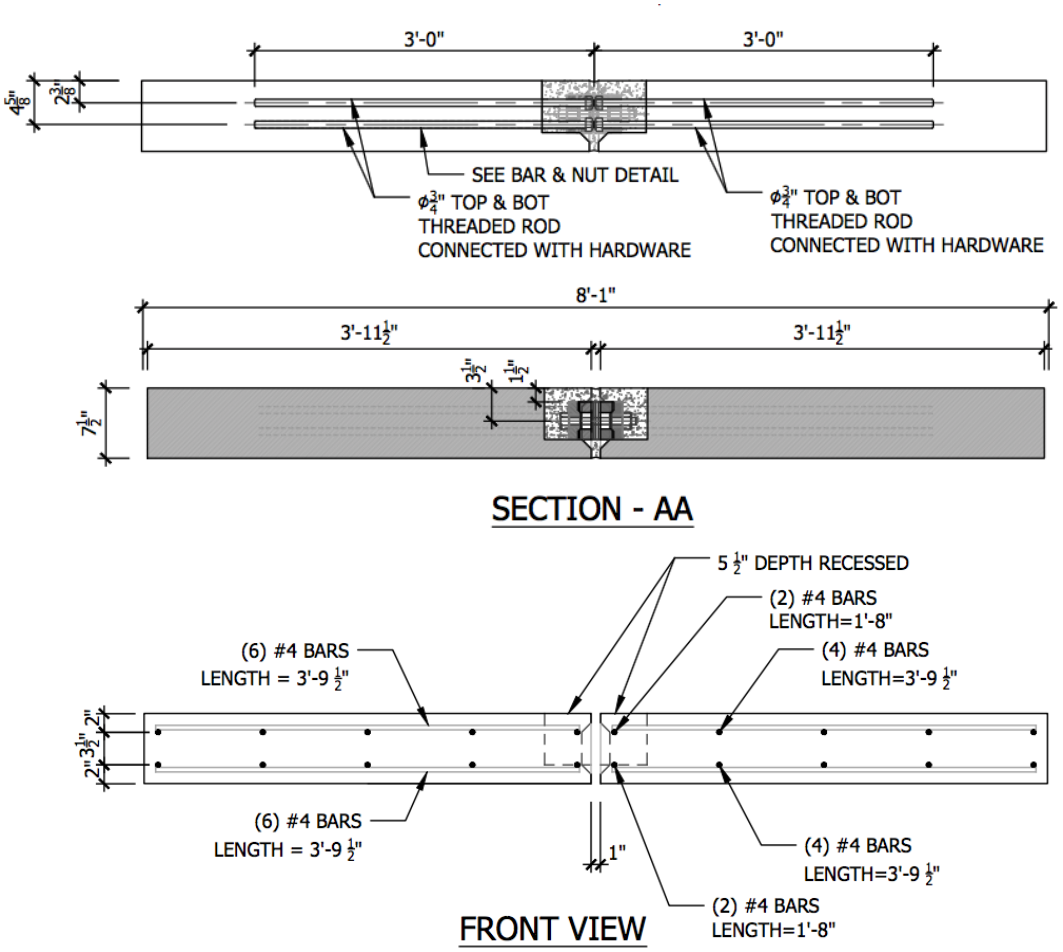

Figure 3.2: Plan and Section View of Slab Specimens Connected

Two types of threaded bars, fine and coarse all-threads, anchoring the mechanical plates to the slab were tested. Five small-scale slab specimens that included these mechanical connections were tested. Two specimens with fine threaded bars, two specimens with coarse threaded bars, and one specimen with a mix of fine threaded bars on one side and coarse threaded bars on the other side were tested.

3.3 Material

3.3.1 Concrete

The concrete was obtained from a local ready-mix supplier (Lyman-Richey Co.). Five specimens were poured with the same mix with one truck which had a target compressive strength of 5,000 psi. Standard compression tests using 6 by 12 in. cylinders were performed to determine the average compressive strength at 7, 14, 21, and 28 days after the cast. The target strength was achieved after 7 days and the average compressive strength at 28 day was 6,790 psi. The strength-gain curve is shown in Figure 3.3 and the test results of the measured strength are provided in Table 3.1.

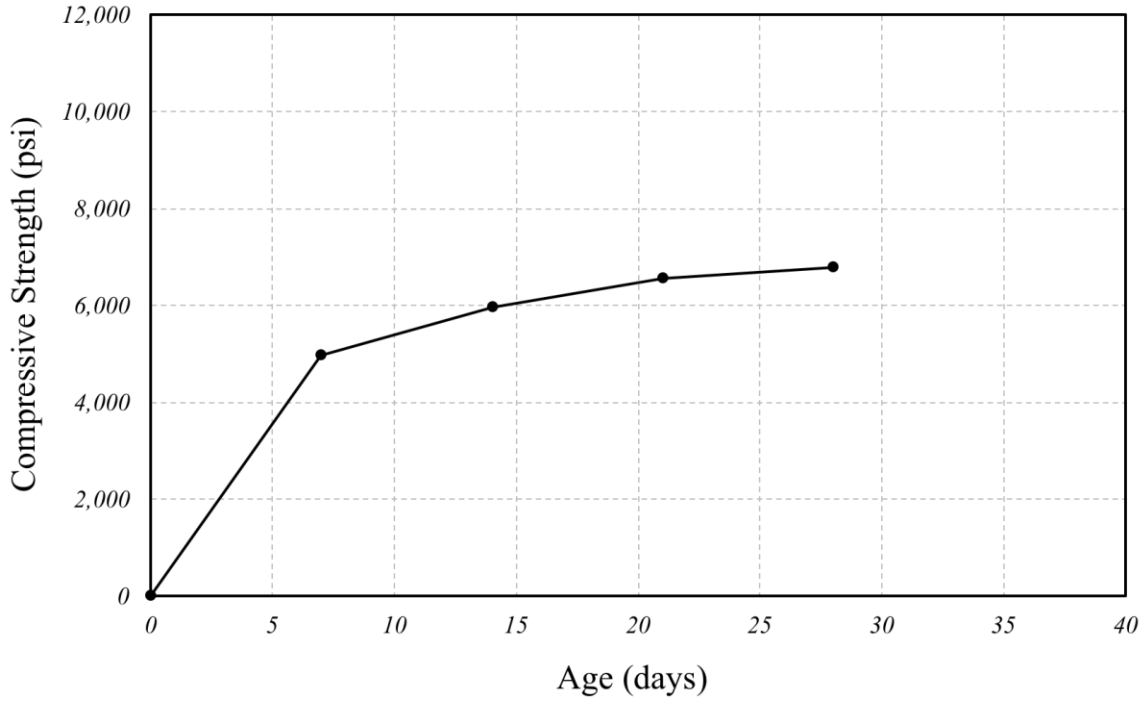

Figure 3.3: Concrete Strength Growth

Table 3.1: Concrete Compressive Strength Data

Maturity	Compressive Strength (psi)	
	Ea.	Avg.
7 (4/27/2017)	5,230 4,520 5,160	4,970
14 (5/4/2017)	5,950 6,050 5,940	5,890
21 (5/11/2017)	6,450 6,780 6,430	6,560
28 (5/18/2017)	6,960 6,690 6,720	6,790

3.3.2 Steel

Conventional Grade 60 steel was used for this project and was provided by Carrol Supply in Council Bluffs, Iowa.

3.3.3 Grout

A non-shrink grout with an expected compressive strength higher than the compressive strength of concrete used for the slab specimens was selected (MasterFlow 928 from the BASF Corporation). Grout specimens were standard 2 by 2 in. cubes per ASTM C109/C109M. These specimens were tested at 3, 7, 14, 21, and 28 days after the pour. The average compressive strength at 28 day was 10,250 psi. The strength-gain curve is shown in Figure 3.4 and the measured data are provided in Table 3.3.

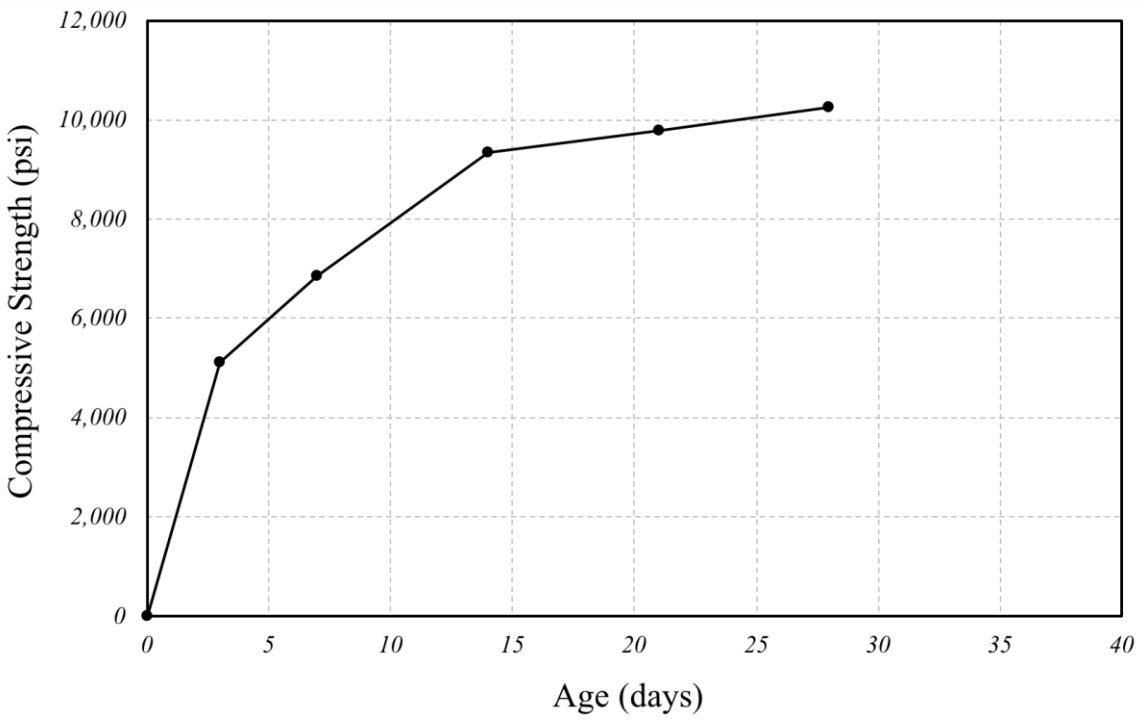

Figure 3.4: Grout Compressive Strength Growth

Table 3.2: Grout Compressive Strength Data

Maturity	Compressive Strength (psi)	
	Ea.	Avg.
3 (4/27/2017)	5,280 5,090 4,970	5,120
7 (5/4/2017)	6,350 6,660 7,550	6,860
14 (5/11/2017)	9,450 8,160 10,440	9,350
21 (5/18/2017)	9,570 9,540 10,200	9,770
28 (5/18/2017)	9,820 10,320 10,590	10,250

3.4 Construction

3.4.1 Formwork

Five platforms were built with each platform providing the formwork for two slabs as shown in Figure 3.5 The base platforms were built with 4 by 8 ft (¾ in. thickness, BC sanded) plywood supported with 2 by 4 in. lumber at 12 in. spacing. The 7.5 in. form walls were constructed out of 4 by 8 ft plywood ripped down to a 7.5 in. height, which is the thickness of the slab specimens. The side walls were reinforced along the bottom by a flat 2 by 4 in. lumber around the entire perimeter. The two slabs were divided by the same plywood and a keyway block out was provided by a 1 by 8 in. board cut to size with 45-degree cuts on each end as shown in the top right photo of Figure 3.5. The divider was built to allow the mechanical joint to be fastened together and ensure the two slab specimens would match up after they are poured. Finally, a block out was built around the mechanical plate, nut, and bolt as shown in Figure 3.5.

It should be noted that the block out around the mechanical joint follows the details provided in Figure 3.2. It should also be noted that these block out designs should be redesigned to allow more space for the removal and replacement of the connection bolt. This was learned after the building experience.

Figure 3.5: Formwork for Mechanical Connection Slab Panels

3.4.2 Casting, Curing, and Storage

All ten slabs were casted on April 20th, 2017 at the Large-Scale Structures Lab located inside the Peter Kiewit Institute at University of Nebraska, Omaha Campus. The concrete was provided by a local ready-mix supplier. Concrete cylinders (6 by 12 in.) were poured with the first concrete to come off of the truck. Seven individuals worked together to pour, place, and finish the specimens. Each slab was finished first with a magnesium trowel and edged. Once the surfaced hardened, each slab was again finished with a steel trowel to get a smooth surface. Around this time in the operation the concrete was ready to have the pick point anchors placed as shown in Figure 3.6.

The slabs were then allowed to rest for around two hours before they were covered with burlap, covered with water, and finally had plastic placed over the top. The same covering process was also used for the cylinders to ensure they had similar curing conditions. For the next seven days after the pour the slabs and cylinders were watered at least once every day and twice when needed to insure the burlap remained saturated. The slabs were then removed from the forms after seven days. The test cylinders were also removed from their plastic forms around the same time. Both the slabs and cylinders were stored in the lab until the test date (Figure 3.7).

Figure 3.6: Finished Slabs After Anchor Placement

Figure 3.7: Slab Panels with Mechanical Joints

3.4.3 Grouting

Each slab was laid together to provide a one-inch gap between the slabs as per the drawings provided in Figure 3.2. The gap width was kept with the help of plastic shims placed in between the metal plates (Figure 3.1). Each mechanical joint was tightened to “snug tight”. Plywood was used to form up the bottoms and ends of the keyway. The slabs were grouted with the MasterFlow 928 as described before.

3.4.4 Transportation

Due to scheduling conflicts at the Large-Scale Structures Lab in PKI (Omaha Campus), it was decided that the slabs would be transported to Lincoln to be tested at the Large-scale Structures Lab at the University of Nebraska-Lincoln Campus. Ayars & Ayars, Inc. provided the transportation of these slabs. Excellent care was taken during loading, transportation, and unloading of the specimens as shown in Figure 3.8.

Figure 3.8: Slab Transportation

3.5 Test Setup and Test Procedure

The testing rig was setup in two separate configurations. The first setup is a four-point bending test with two supports placed at the far ends of the specimen and two spreader beams were placed on either side of the joint 9 in. from the center. Rollers were placed at all four contact points and a rubber pad was provided between the slab specimen and roller loading plates as shown in Figure 3.9. Load cells were used to measure the loads applied. String potentiometers were used to measure the displacement and six of these sensors were placed on each side of the specimen as shown below.

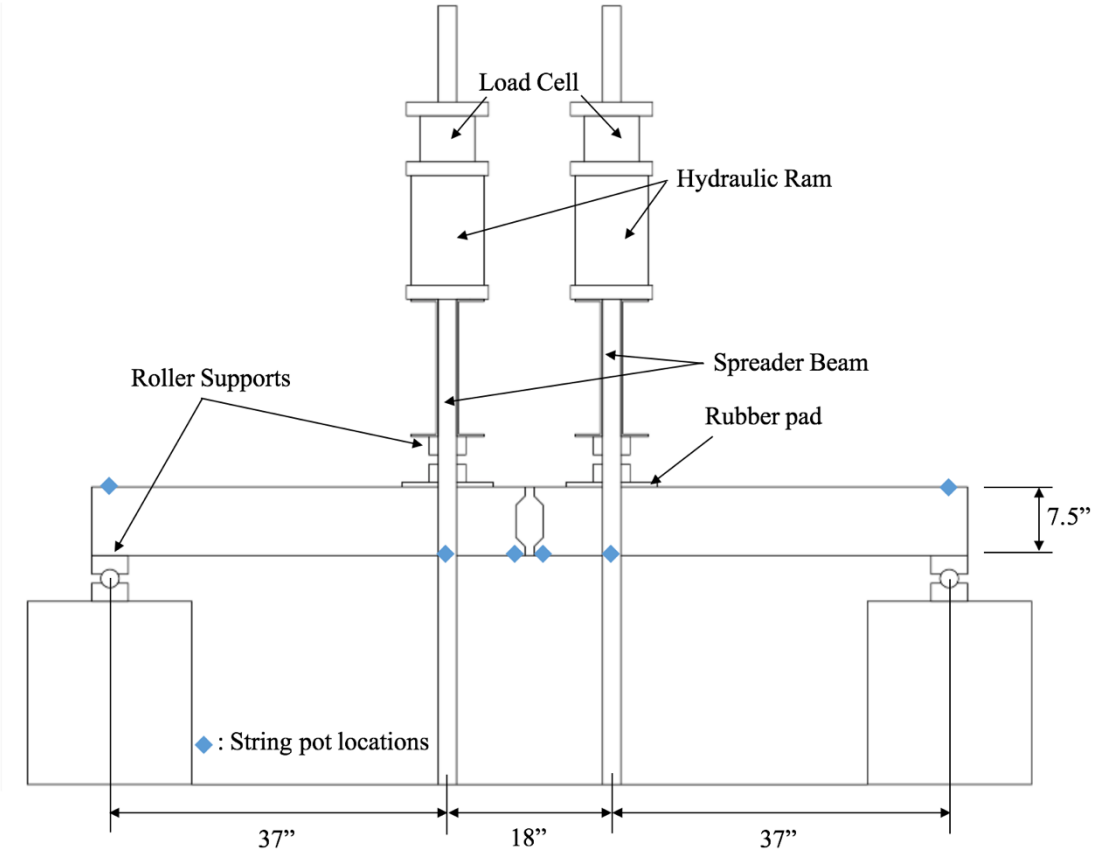

Figure 3.9: Four-Point Bending Test Setup

The second configuration for three-point bending consists of the same locations for the support but the center of loading placed 2.5 in. from the center of the slab as shown in Figure 3.10. For the three-point bending test both load cells were placed on the spreader beam on each side of the rods where load was applied. Four string potentiometers were placed on each side of the specimen as shown in Figure 3.10.

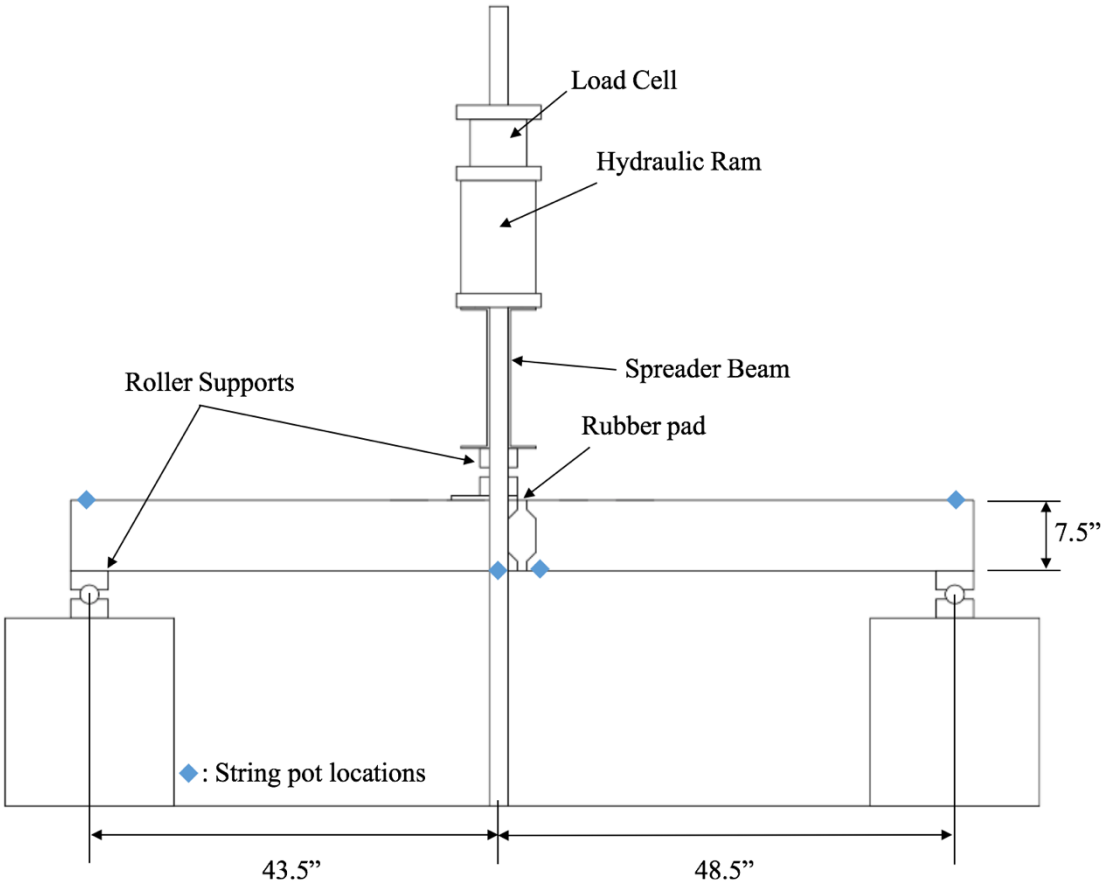

Figure 3.10: Three-Point Bending Test Setup

For both the three-point and four-point bending tests the same basic procedures were used. Each specimen was lifted into place and set squarely on the supports. At this point all the hooks for the string pots were placed with adhesive to the specimen. The spreader beams were

then lifted as an assembly and placed on the specimen. Hydraulic lines were hooked up and the data acquisition system was checked to make sure sensors were reading correctly. Force was applied through a hydraulic pump. Load was continually added in a small increment (0.5-1 kip) until there was a significant drop in the load capacity of the specimen.

3.6 Test Results

3.6.1 Specimen F-F-1

This section provides the test results of four-point bending test on the specimen containing fine all-threads on each side (Specimen F-F-1, Figure 3.11). The first crack was observed at the interface between the grout and the specimen as shown in Figure 3.12, which was also within the constant moment region where the moment was the highest.

Figure 3.11: Four-point Bending Test Setup (Specimen F-F-1)

Figure 3.12: Initial Cracking at the Grout Interface (Specimen F-F-1)

As more load was applied, the crack at the interface opened up at the bottom allowing rotation and eventually crushed the concrete on the top part of the slab as shown in Figure 3.13, and the grout can be seen eventually pulling away from the concrete on the bottom side at failure from a close-up photo (Figure 3.14). The load-displacement curve for Specimen F-F-1 is shown in Figure 3.15. The maximum load reached was 8.5 kips on one side of the slab (from two hydraulic rams) and the deflection at peak load was 1.6 in. The test was terminated when there was an obvious drop in the load-displacement curve as shown in Figure 3.15 and the slab was not able to take more load but deflection was increasing due to the rotation at the joint. Considering the reading at failure load from the two load cells which were 8.5 kips, the spreader beam weight under the hydraulic ram which was 2 kips, and including the moment caused by the self-weight (4.6 kip-ft), the total experimental joint moment was 37 kip-ft.

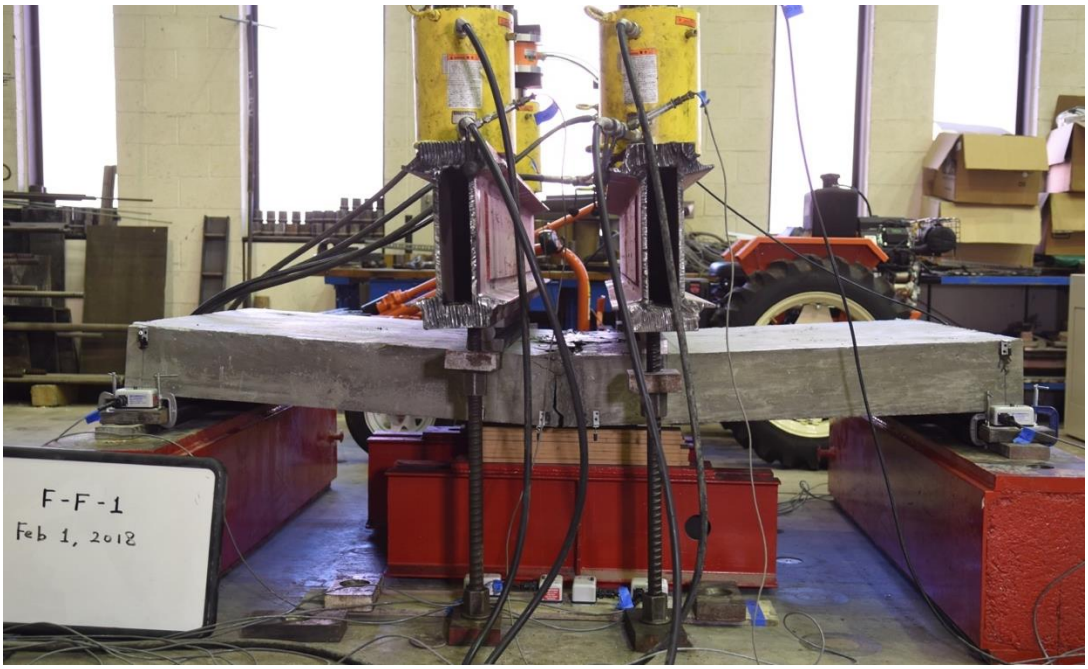

Figure 3.13: Concrete Crushing at Top (Specimen F-F-1)

Figure 3.14: Grouted Joint Close-up Photo at Failure (Specimen F-F-1)

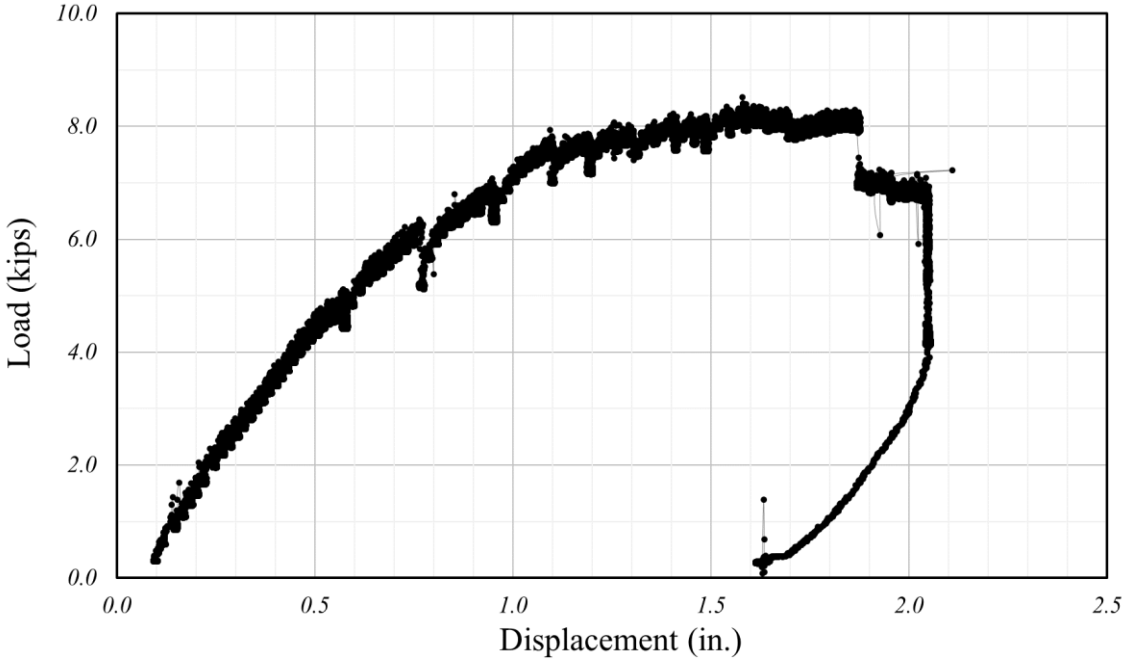

Figure 3.15: Load-Displacement Curve (Specimen F-F-1)

Figure 3.16 shows a close-up photo of the joint taken after the test was complete. Other than the shear crack that initiated at the corner of the joint where the shape changes that propagated through the slab to the loading points and some cracks initiating from the corners of the block out area, no other cracks were observed in the two slabs connected. The grout was taken out after the testing was complete to observe the performance of the mechanical joint after failure. As shown in Figure 3.17, the two slabs were still connected by the ASTM A490 bolt through the mechanical joint. All fine threaded bars were embedded in concrete well.

Figure 3.16: Specimen F-F-1 Joint Close-up Photo after Failure

Figure 3.17: Mechanical Joint Connecting the adjoining Slabs after Failure

3.6.2 Specimen C-C-1

This section provides the test results of the four-point bending test on the specimen containing coarse all-threads on each side (Specimen C-C-1, Figure 3.18). The first crack was observed at a similar location as shown in Specimen F-F-1 at the interface between the grout and the specimen in the south side (front). However, on the north side (back), as shown in Figure 3.19, the crack that initiated from bottom started to shear through the grouting. As more load was applied, the crack propagated in an inclined direction towards the loading point as shown in Figure 3.20. The crack at the joint opened up wide allowing the two slabs to rotate until the top of the grout crushed (Figure 3.21). However, the top of the concrete slab did not crush as much as Specimen F-F-1.

Figure 3.18: Four-point Bending Test Setup (Specimen C-C-1)

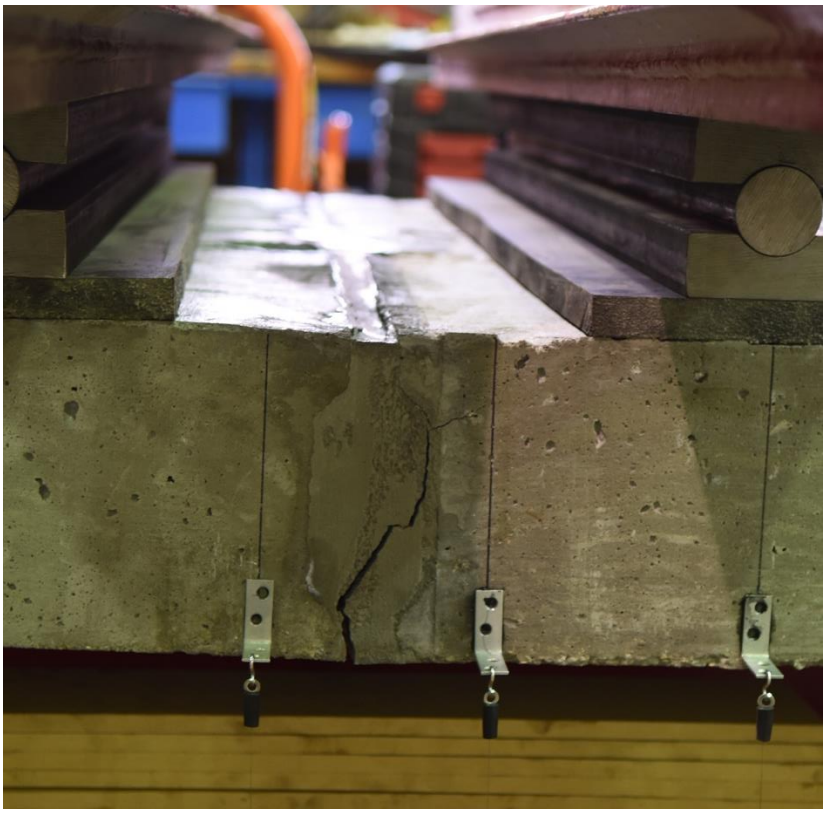

Figure 3.19: Initial Cracking through the Grout (Specimen C-C-1)

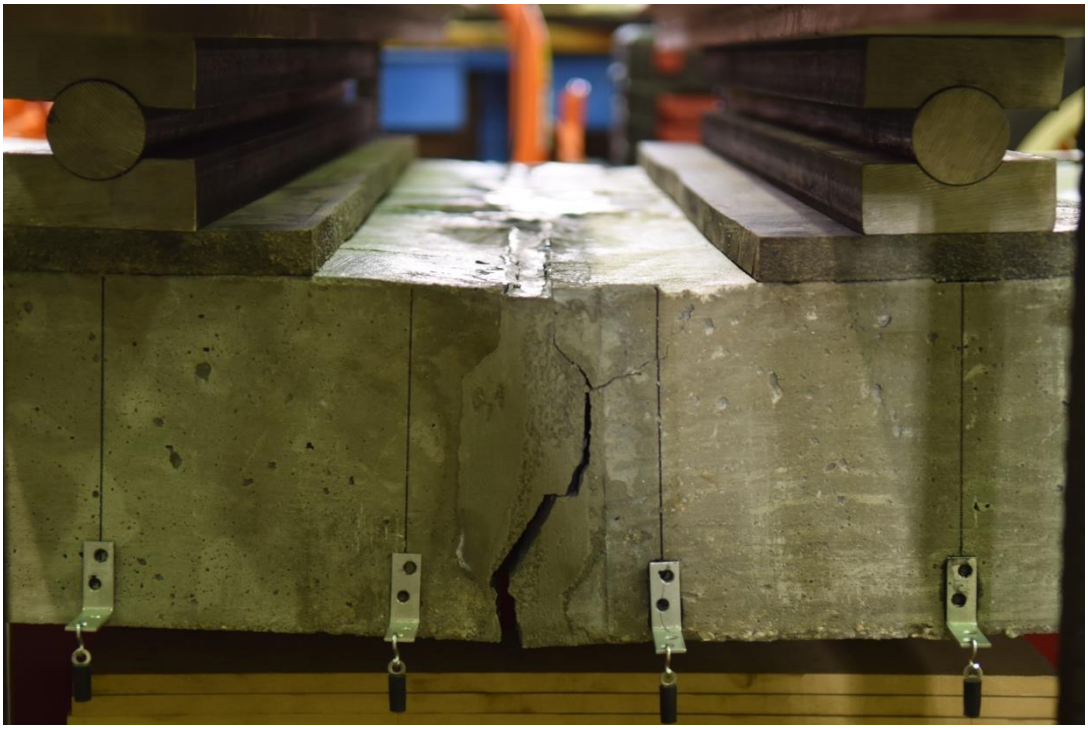

Figure 3.20: Crack Propagation through the Grout (Specimen C-C-1)

Figure 3.21: Specimen C-C-1 at Failure (view from South side)

Figure 3.22: Specimen C-C-1 at Failure (view from North side)

Figure 3.23 is the load-displacement curve for Specimen C-C-1. The maximum load reached was 8.4 kips and the deflection at the peak load was 1.46 in. The test was terminated when there was a significant drop in the load and the slab were not able to take more load but deflection was increasing due to the rotation at the joint. As shown in Figure 3.23, although the maximum load was similar to Specimen F-F-1, the load drop occurred at a deflection less than the case with F-F-1 and there was large rotation at failure as shown in Figure 3.22. This is probably the reason crushing was mainly seen in the grouting rather than the concrete slab. It is also possible that the fine threads bond better than the coarse threads and this may be the reason there are less obvious cracks around the block out area. Considering the reading of the failure load from the two load cells was 8.4 kips, the spreader beam weight under the hydraulic ram was

2 kips, and including the moment caused by the self-weight (4.6 kip-ft), the total experimental joint moment was 36.6 kip-ft.

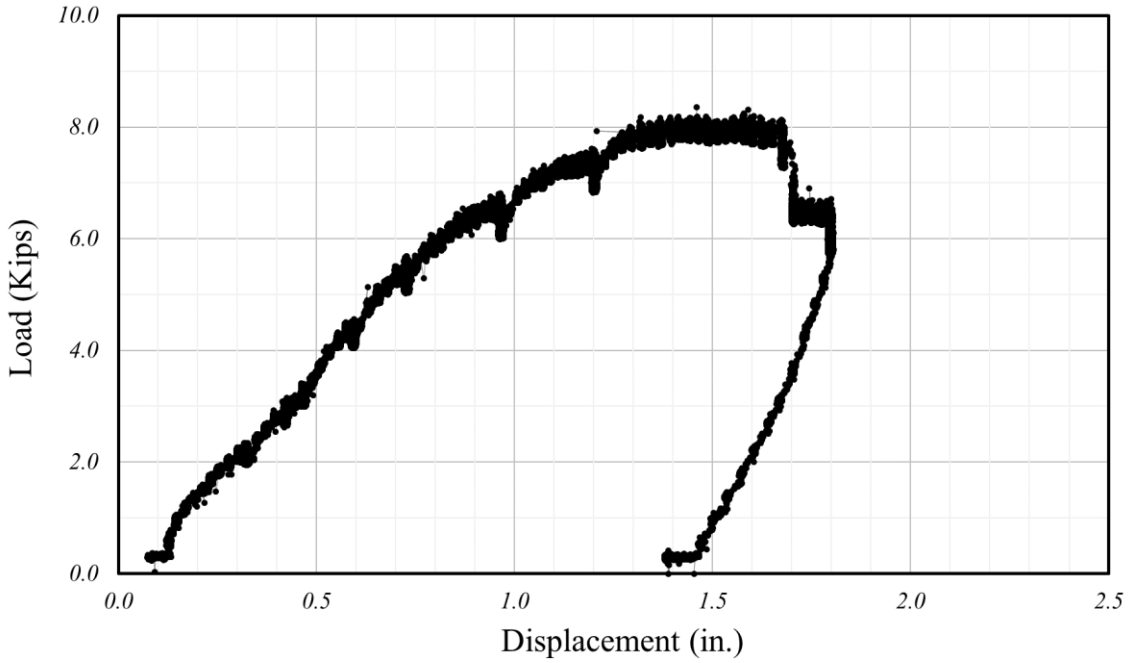

Figure 3.23: Load-Displacement Curve (Specimen C-C-1)

After the test was complete, all the grout was taken out to check the mechanical connection. The coarse threaded bars were noted to have sheared off as shown in Figure 3.24. This was possibly caused by less bond of the coarse threads compared to the fine threaded bars. If the threaded bars were slipping near failure, there is a possibility that all the moments were taken by these threaded bars before failure, which is the reason Specimen C-C-1 was not able to take more rotation and the load capacity dropped suddenly at a smaller deflection value than Specimen F-F-1.

Figure 3.24: Mechanical Joint Shear Failure (Specimen C-C-1)

3.6.3 Specimen C-F-1

This section provides the test results of the four-point bending test that was conducted on the specimen containing fine all-threads on one side and coarse all-threads on the other side (Specimen C-F-1, Figure 3.25). Initial cracking was shown at the interface between the slab and the grouting similar to other specimens as shown in Figure 3.26. This crack shown in the interface opened larger as more load was applied. And, as load increased, the crack at the interface started to propagate in an inclined direction starting from where the shape of the grout shear key changes towards the loading point as shown in Figure 3.27. There was no crack through the grout as shown in the case with Specimen C-C-1. The top of the grouting crushed before failure as shown in Figure 3.28.

Figure 3.25: Four-point Bending Test Setup (Specimen C-F-1)

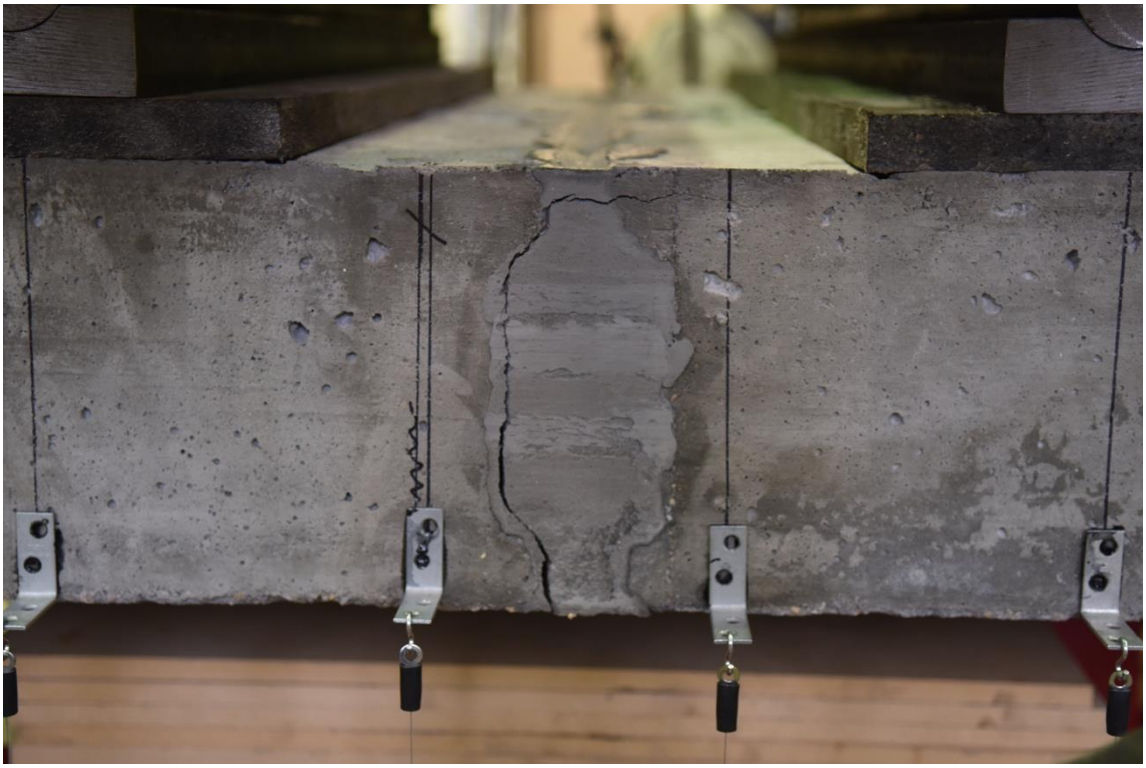

Figure 3.26: Initial Cracking at the Grout Interface (Specimen C-F-1)

Figure 3.27: Crack Propagation (Specimen C-F-1)

Figure 3.28: Specimen C-F-1 at Failure

The load-displacement curve for Specimen C-F-1 is shown in Figure 3.29. The maximum load reached was 7.8 kips and the deflection at peak load was 1.2 in. The test was terminated when there was an obvious drop in the load-displacement curve as shown in Figure 3.29 and the slab was not able to take more load while deflection was increasing due to the rotation at the joint. Considering the reading at failure load from the two load cells which was 7.8 kips, the spreader beam weight under the hydraulic ram which was 2 kips, and including the moment caused by the self-weight (4.6 kip-ft), the total experimental joint moment was 35 kip-ft. This was the specimen that carried the least load. It is interesting to note that although the load dropped earlier, unlike Specimen C-C-1, this specimen was able to rotate and deflect more than C-C-1. The load-displacement curve does look like a combination of the curves shown for Specimen F-F-1 and C-C-1.

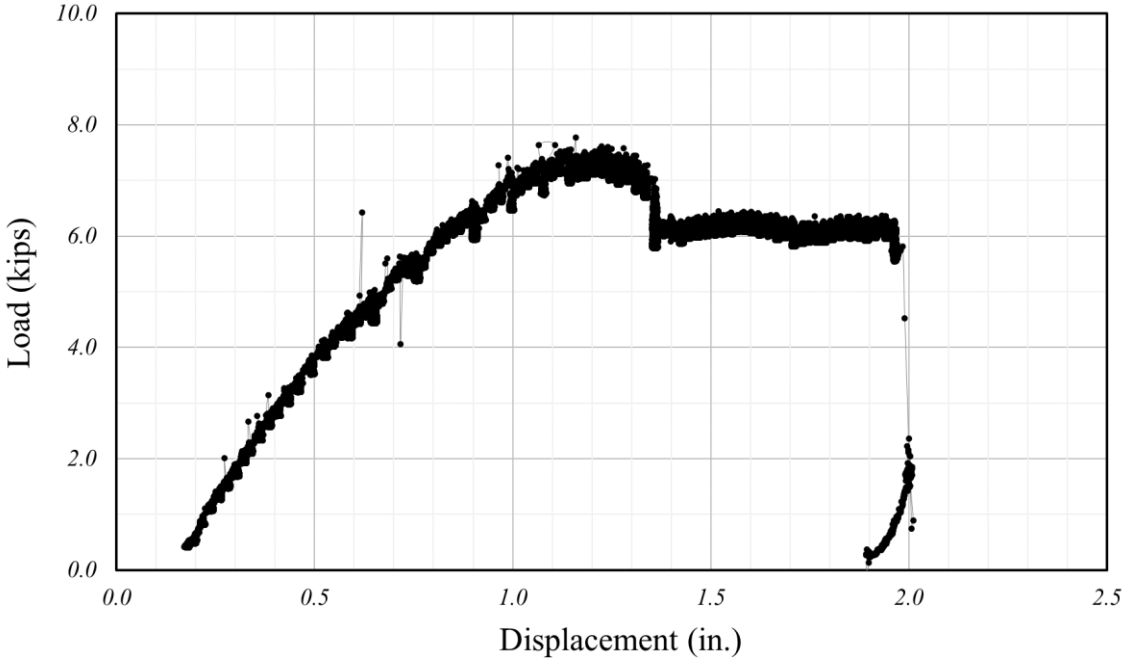

Figure 3.29: Load-Displacement Curve (Specimen C-F-1)

3.6.4 Specimen C-C-2

This section provides the test results of the three-point bending test that was conducted on the specimen containing coarse all-threads (Specimen C-C-2, Figure 3.30). Initial cracking was seen at the interface between the slab and the grout similar to other specimens as shown in Figure 3.31. This crack shown at the interface opened larger as more load was applied. As load increased, the crack at the interface started to propagate in an inclined direction starting from where the shape of the grout shear key changes towards the loading point as shown in Figure 3.32.

Figure 3.30: Three-point Bending Test Setup (Specimen C-C-2)

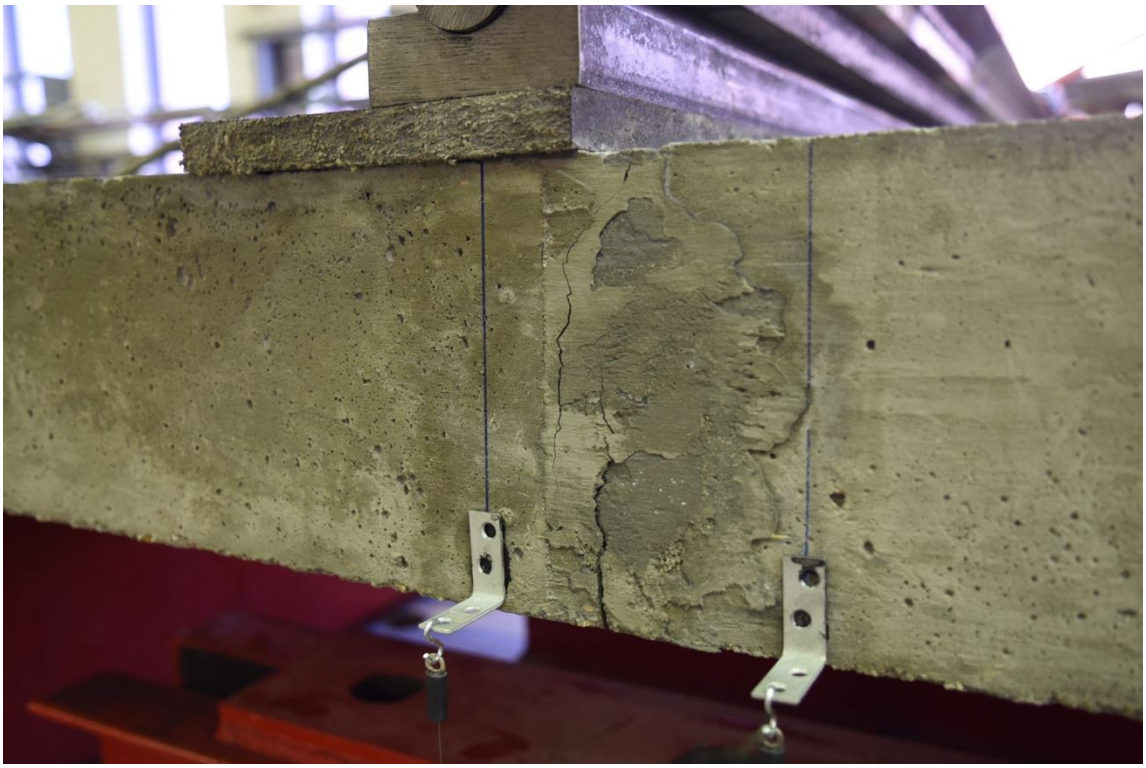

Figure 3.31: Initial Cracking at the Grout Interface (Specimen C-C-2)

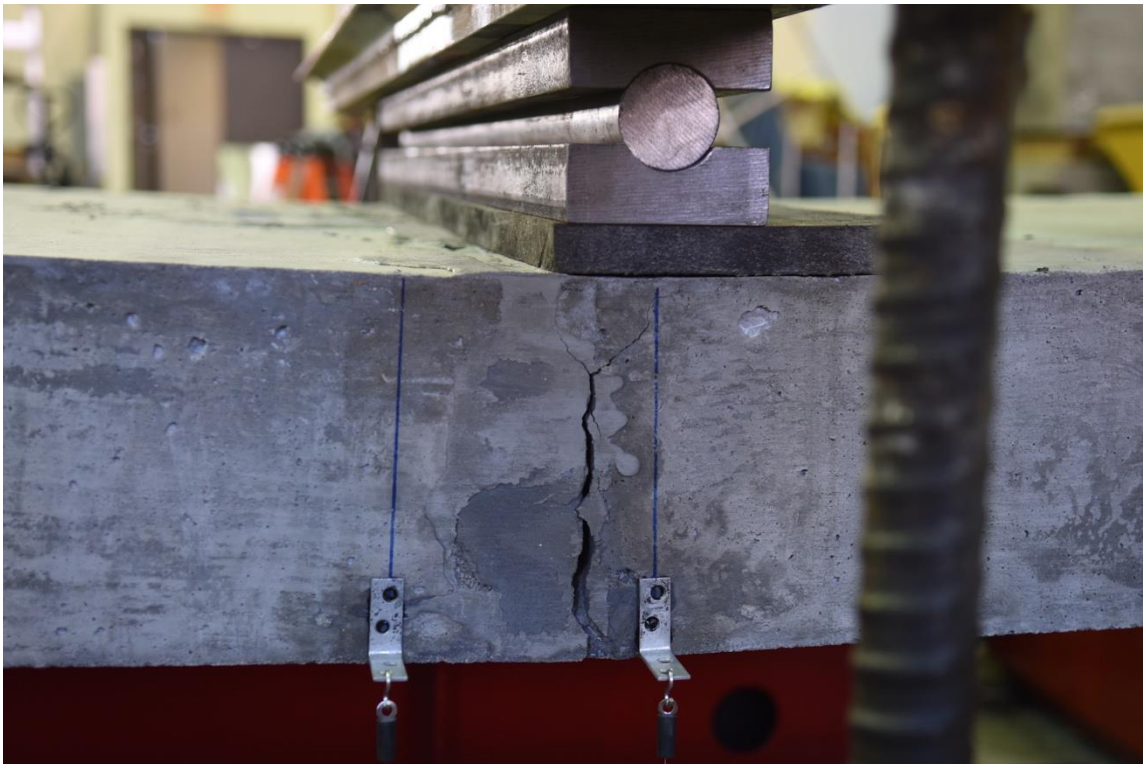

Figure 3.32: Crack Propagation (Specimen C-C-2)

Figure 3.33: Specimen C-C-2 at Failure

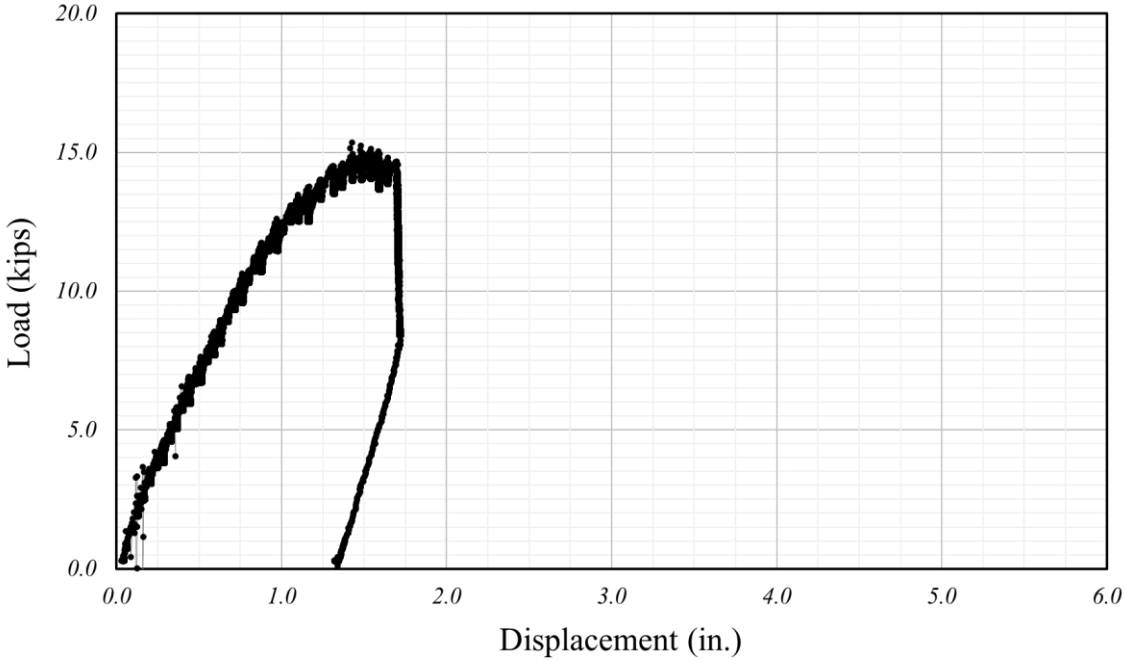

Figure 3.34: Load-Displacement Curve (Specimen C-C-2)

The failure mode was relatively more brittle in this test compared to the identical specimen tested in four-point bending. There was not much crushing seen in the grout or the concrete slab at failure but rather a huge gap at the interface between the shear key and the slab that was loaded as shown in Figure 3.33. The load-displacement curve for Specimen C-C-2 is shown in Figure 3.34. The maximum load reached was 15.4 kips and the deflection at peak load was 1.4 in. Unlike the four-point bending tests, the load dropped suddenly and it was not possible to see further deflection due to rotation (without further load increase). The shear span for this test was rather slender (a/d = 5.8) where it is known that the member fails at a disrupt inclined cracking load. The reading at failure load from the two load cells was 15.4 kips and the reaction force at each support would be 7.7 kips. Considering that the spreader beam weight under the hydraulic ram was 2 kips and including the moment caused by self-weight (5.4 kip-ft) of the slab, the total experimental joint moment was 36.9 kip-ft.

3.6.5 Specimen F-F-2

This section provides the test results of the three-point bending test that was conducted on the specimen containing fine all-threads (Specimen F-F-2, Figure 3.35). Initial cracking was shown at the interface between the slab and the grout and inside the grout key as shown in Figure 3.36. As load was increased, it is interesting to note that there was an inclined shear crack through the grout as shown in Figure 3.37. This crack was inclining towards the loading point. As additional load was applied, these cracks opened wider and an additional inclined shear crack was observed as shown in Figure 3.38. The close-up photo of the joint taken from the North side of the specimen indicates that the grout key as a whole is about to fall out from the joint before failure (Figure 3.39).

Figure 3.35: Three-point Bending Test Setup (Specimen F-F-2)

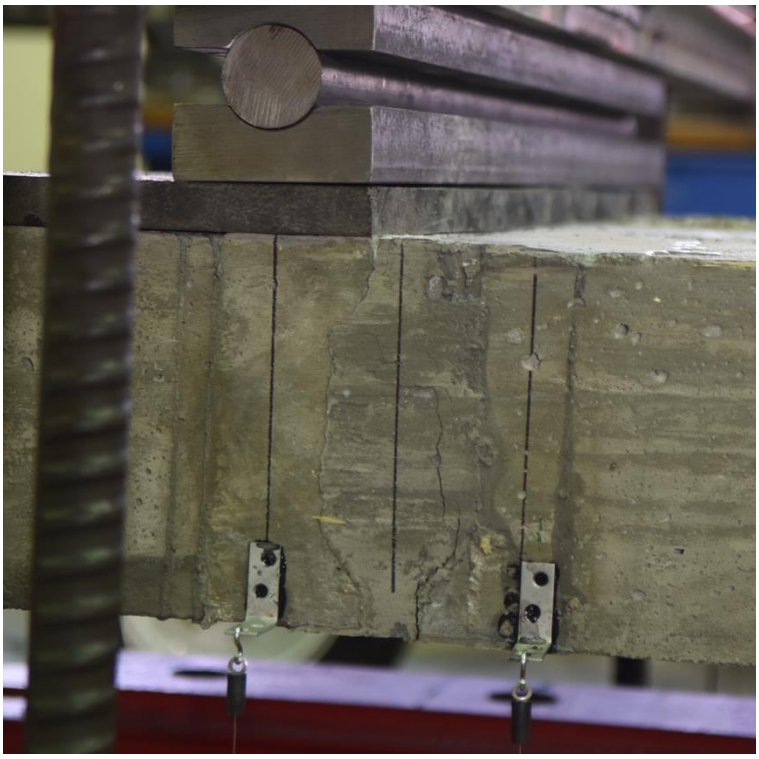

Figure 3.36: Initial Cracking at the Grout (Specimen F-F-2)

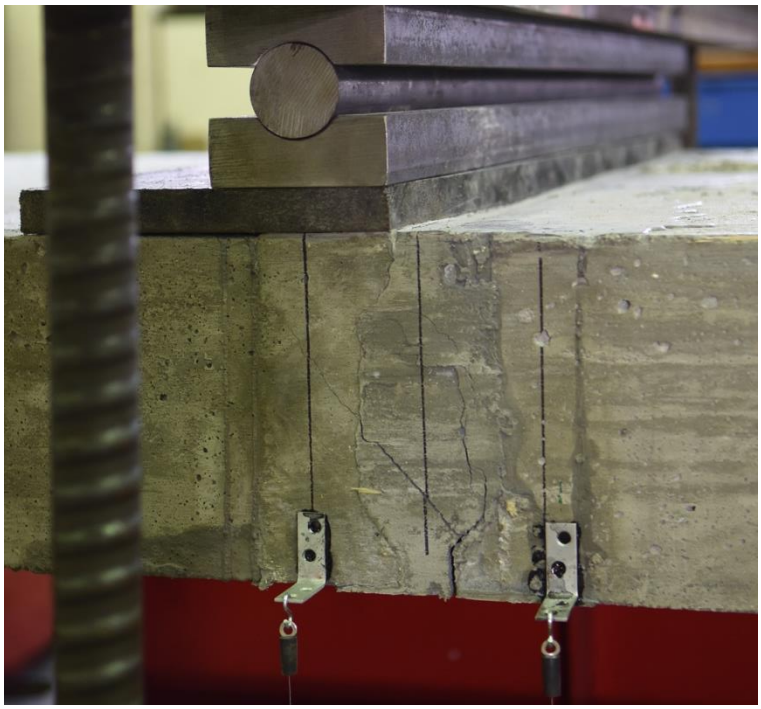

Figure 3.37: Inclined Cracking through the Grout (Specimen F-F-2)

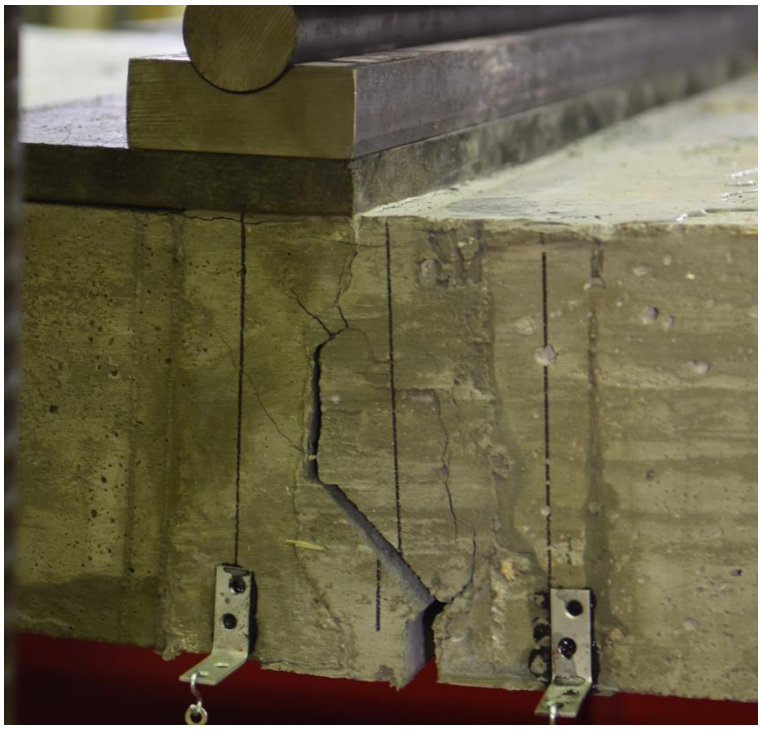

Figure 3.38: Grout Joint Close-up Photo (Specimen F-F-2, South view)

Figure 3.39: Shear Key before Failure (Specimen F-F-2, North view)

The failure mode was similar to Specimen C-C-2 and relatively more brittle compared to the identical specimen tested in four-point bending (Figure 3.40), showing a sudden drop in load. However, the load-displacement curve shown in Figure 3.41 demonstrates that Specimen F-F-2 reached to a higher load and deflected more than what was seen in Specimen C-C-2. The maximum load reached was 18.3 kips and the deflection at peak load was 3.8 in. The reading at failure load from the two load cells were 18.3 kips providing a reaction force at each support of 9.15 kips. Considering that the spreader beam weight under the hydraulic ram was 2 kips and including the moment caused by self-weight (5.4 kip-ft) of the slab, the total experimental joint moment was 42.2 kip-ft.

Figure 3.40: Specimen F-F-2 at Failure

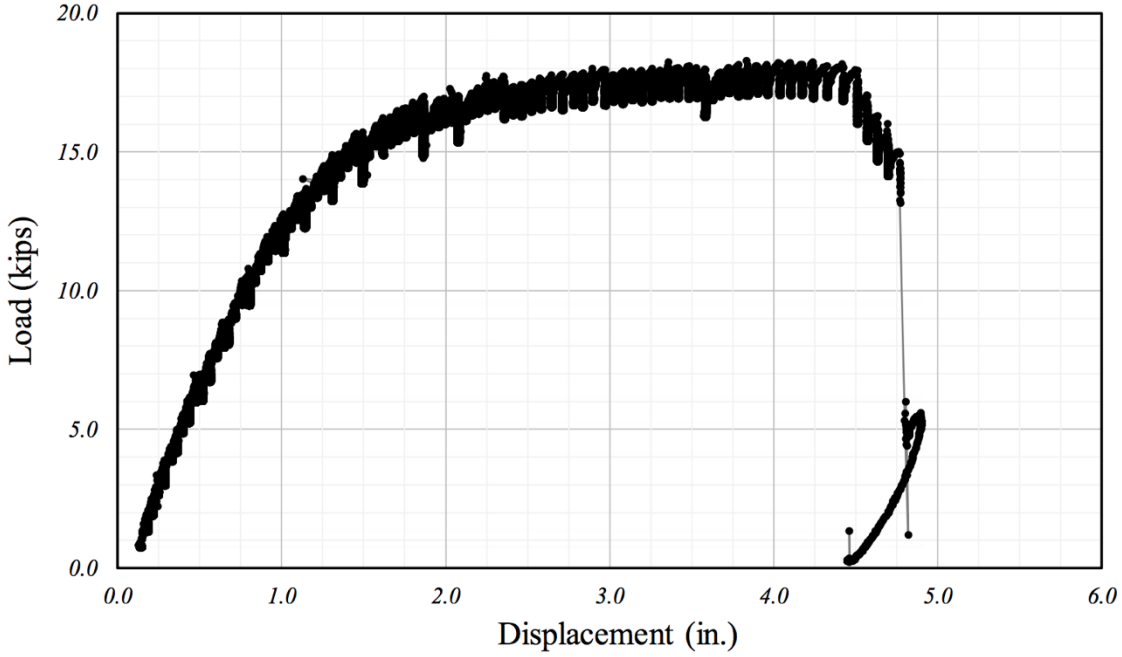

Figure 3.41: Load-Displacement Curve (Specimen F-F-2)

3.7 Summary

Ten slabs were casted to evaluate the joint capacity of five connected slab specimens. A new type of mechanical joint system for precast adjacent beams was proposed. This mechanical joint which is comprised of four all threads with nuts, an alignment plate, an anchor plate, and a 1.25 in. ASTM A490 bolt with a nut that can connect the deck portion of the precast adjacent beams. Threaded bars with fine threads, coarse threads, and a mix of each of them were tested. The threaded bars with fine threads had the best performance. It was noted that although the joint did not carry more moment after exceeding the capacity, it did allow additional rotation to take place. After completion of the testing, the grouted keys were demolished to check the mechanical connections, and for the case with fine threaded bars, the mechanical joint was holding the adjoining slab specimens together. The following table is a summary of the moment

and shear strengths of each specimen. On average, the experimental joint moment was 37.5 ft-kip and the tested joint shear was 16.6 kip.

Table 3.3: Experimental Joint Moment and Total Load Applied

Specimen	**Experimental Joint Moment (ft-kip)**	**Total Load Applied (kips)**
F-F-1	37.0	17.0
F-F-2	42.2	18.3
C-C-1	36.6	16.8
C-C-2	36.9	15.4
C-F-1	35.0	15.6
Avg.	**37.5**	**16.6**

CHAPTER 4. FULL-SCALE TEST PROGRAM

4.1 Introduction

The objective of this phase of research is to investigate the shear and moment capacity of the new type of mechanical connection that was tested in small-scale as a proof of concept, in full-scale with the cross sections that would be used in the field. In this phase of research, a single full-scale formwork was constructed which allows to build multiple sections including a 1) 8 ft wide section that is 1 ft deep, which is similar but wider than the plank sections that are currently being used in Nebraska counties, 2) 8 ft wide section that is 2 ft deep, which can span up to 50 ft, and 3) 8 ft wide section that is 3 ft deep, which can span up to 60 ft. One formwork will allow casting all three sections which may serve most of the Nebraska county bridges applications.

For this testing program, 8 ft wide, 2 ft deep cross section which can span up to 50 ft was cast and divided into five 10 ft long specimens to test out multiple types of joints. Five sets of these specimens were cast. One set of these 10 ft long sections was connected with a mechanical connection proposed in Chapter 3. In addition to the mechanical joint with self-consolidating concrete grout, a staggered rebar splice joint grouted with a commercial mix of ultra-high-performance concrete, new types of Nebraska fiber-reinforced high-performance concrete, a new type of super high-performance concrete, and a ultra-high-performance concrete was tested additionally to evaluate various types of joint systems.

4.2 Specimen Design

Each specimen was a 10 ft long T-beam that measured 8 ft wide and had a 28.5 in. deep, 14 in. wide stem as shown in Figure 4.1. The top flange depth was 7.5 in. Shear keys were

provided along the length of each specimen and a total of five specimens were cast together. A second pour followed to create the adjoining specimens. All specimens had a top and bottom mat of No. 4 bar while the stem had 8 No. 11 bars at the bottom. No. 4 stirrups were provided as transverse reinforcement. All bars were high-strength ChromX 9100 bars from MMFX Technologies with a yield strength of 130 ksi.

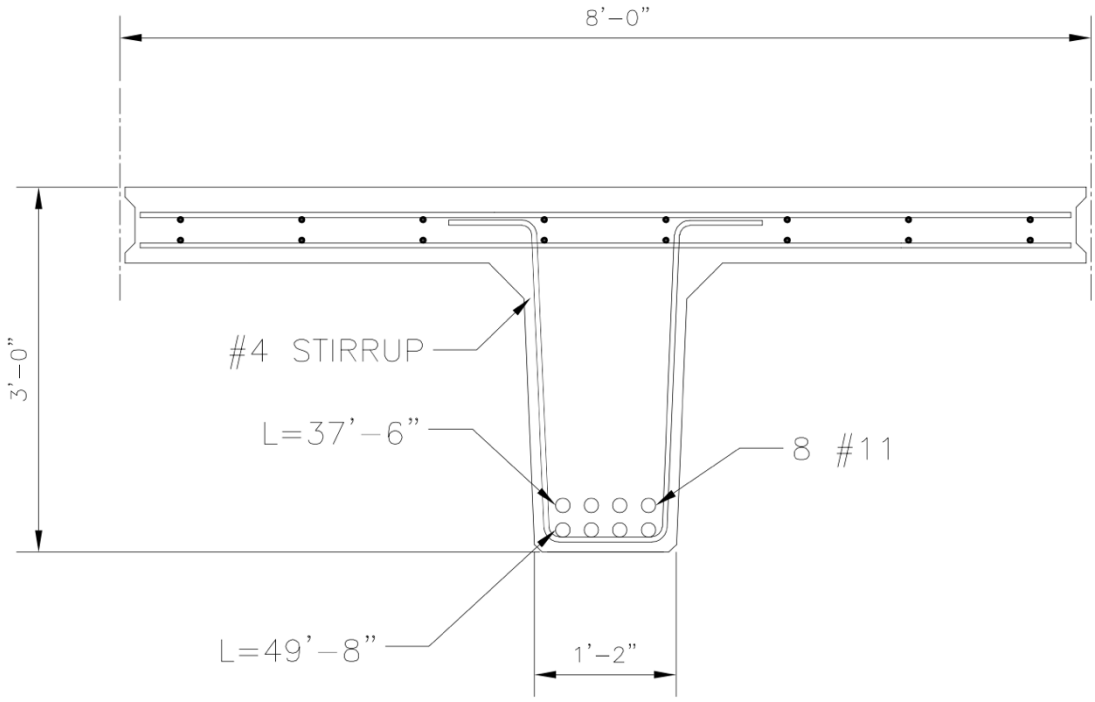

Figure 4.1: Cross Section of Full-Scale Specimens

4.3 Material

4.3.1 Concrete

The concrete was obtained from a local ready-mix concrete supplier (Lyman-Richey Co.). For each pour, three trucks were required to cast the five specimens and forty-two 6 by 12 in. cylinders which had a target compressive strength of 6,000 psi. Self-consolidating concrete was used for the pour for the ease of construction. The mix contains ½ in. aggregates (UNO

SCC 0.5 LS Mix from Lyman Richey Co.). Standard compressive and splitting-tensile tests for 6 by 12 in. cylinders were performed at 3, 7, 14, 21, and 28 days after testing.

4.3.2 Steel

ChromX 9100 bars from the MMFX Technologies was used for the reinforcing steel bars which had a typical yield strength of 130 ksi. The reason high-strength reinforcement was used in this study is because based on a feasibility study conducted by e-Construct (local engineering firm in Omaha) it was noted that the span length when using this reinforcement for short span bridges is comparable to having prestressing strands and the span length can increase up to 20-30 % with the identical cross section using convention Grade 60 steel. The possibility of using ChromX 9100 steel bars as an alternative to the strands in this design was one of the expected benefits for the newly proposed precast bridge section.

4.4 Construction

4.4.1 Formwork and Steel Assembly

The formwork for these specimens was built by a specialized contractor (Hunt Construction) and was shipped to the Large-Scale Structures Lab at Peter Kiewit Institute at the University of Nebraska-Omaha Campus. All formwork was shipped in partially pre-fabricated 8 ft segments as shown in Figure 4.2. The specialized contractor built the stem walls, side walls, flange forms, and supports for the side of the flange.

Figure 4.2: Formworks for Full-Scale Bridge Specimens

A base of 4 by 8 ft (3/4 in. thickness) plywood supported by 2 by 4 in. studs was built to cover a 12 ft by 56 ft lab space. The stem walls were then secured to this base and kickers were used to secure the top of the stem wall. The flange form was then attached to the stem wall form.

The side walls were attached to the flange form and the kickers were placed between the platform base and the top of the side wall forms to secure the top as shown in Figure 4.3. Dividers were then installed along the length of the full form to create five 10 ft sections. The complete assembled formwork with diagonal supports is shown in Figure 4.4.

Figure 4.3: Full-Scale Formwork Assembly

Figure 4.4: Complete Full-Scale Formwork for County Bridge Specimen

All steel bars were tied by the research team consisting of graduate students and faculty members. No. 11 longitudinal bars which were placed in the stem were built outside the formwork with No. 4 transverse reinforcement tied together. The reinforcement cage was then dropped into the stem using the overhead crane. Top and bottom mat of No. 4 bars were placed as deck reinforcement to finalize the work. Figure 4.5 shows a photo of the assembled steel reinforcement placed inside the entire formwork.

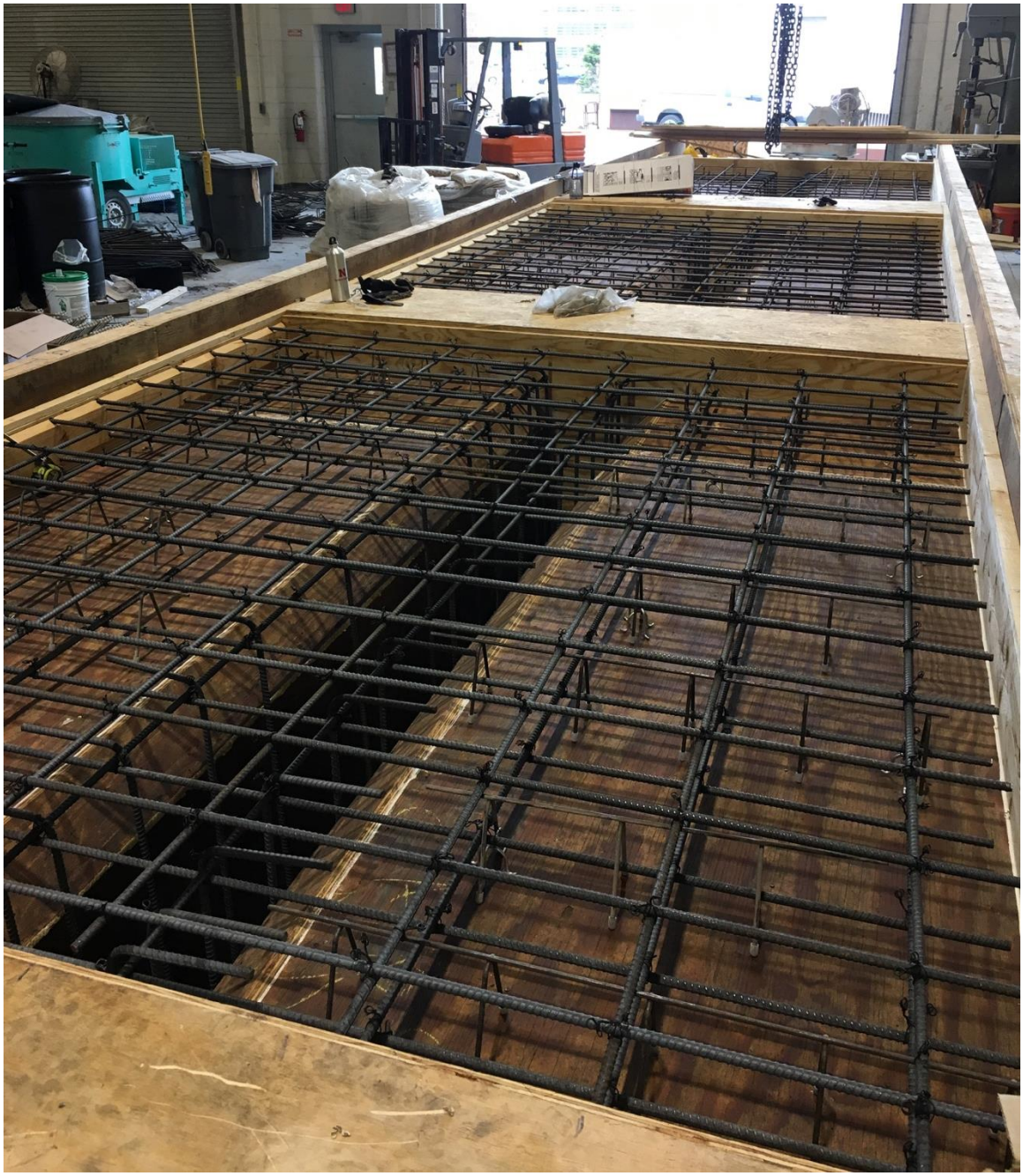

Figure 4.5: Steel Reinforcement Assembly Placed in Formwork

For the mechanical joint system introduced in Chapter 3, the design was slightly changed to incorporate a Nelson stud shear connectors welded 45 degrees to the plate (Figure 4.6) spanning out in longitudinal direction instead of having threaded bars. The reason, the mechanical joint system tested in Chapter 3 was not used in this case was due to the threaded bar

material availability at the time of testing. A block out was built around the plates on the side walls. For specimens that were planned to have high performance fiber-reinforced concrete, super high-performance concrete, or ultra-high-performance concrete in the shear key, holes were drilled through the side walls so that the reinforcing bars could pass through creating a staggered rebar splice joint.

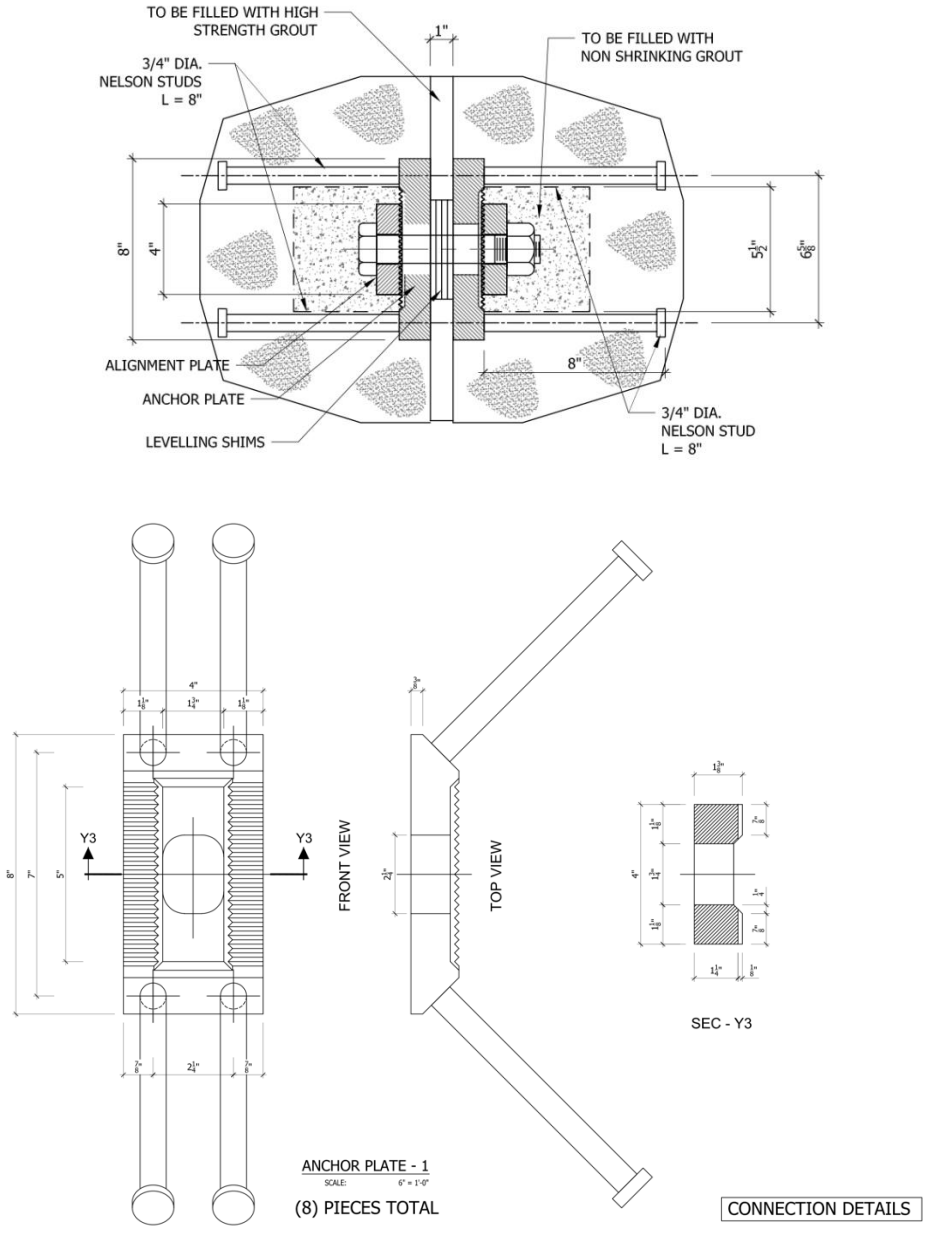

Figure 4.6: Mechanical Joint with 8 in. Nelson Studs

4.4.2 Casting, Curing, and Storage

The following procedure described in this section was identical for both pours with three trucks used in each case. Two people ran the chute and raked concrete while two other people ran the screed board. While this process was going on six people filled the test cylinders for all three trucks. The process was relatively simple with the use of self-consolidating concrete.

Figure 4.7: Casting Self-Consolidating Concrete for Full-Scale Bridge Specimens

After the concrete was poured the casting crew waited until the concrete started to set up and ran a bull float over every specimen while also edging as shown in Figure 4.8. The team then waited another 45 minutes to set anchors in all four corners of each of the specimen. After the anchors were set and two hours had past, burlap and plastic sheeting was placed on top of the

specimens for curing. Water was applied right before the plastic was placed and re-applied every day for the next seven days. After these seven days, the specimens were removed and the formwork and steel reinforcement assembly were prepared for the second pour as shown in Figure 4.9. The test cylinders were all capped after they were filled and removed from the forms after seven days to mimic the environment of the actual bridge specimen. All the specimens were kept inside the lab until the test program could commence.

Figure 4.8: Finishing the Full-Scale Bridge Specimens

Figure 4.9: Steel Assembly for the Second Pour

Figure 4.10 shows one of the precast sections taken out from the formwork. As of special note, unlike the concerns of the stability of these cross sections, due to the fact that the bottom stem was 14 in. wide and only 28 in. deep, the specimen was standing with no further support required. Figure 4.11 shows the specimens in storage. These specimens will have staggered splice joint. Considering that No. 4 bars were used for the deck reinforcement, the required splice length for conventional concrete to develop 60 ksi in a 6,000 psi concrete would be approximately 30 bar diameters. This would require 15 in. development length. As shown in Figure 4.11, note that the splice length is much shorter than what would be typically be required at these joints. This was made possible by the use of the high-performance concrete placed in shear keys.

Figure 4.10: Proposed Standard County Bridge Section after Construction

Figure 4.11: Test Specimens with Short Splice Length

4.5 Test Setup and Test Procedure

The testing rig was setup for a three-point bending test with a hydraulic ram placed in the middle of the specimen and supports at the two ends of the specimen as shown in Figure 4.12. However, since two specimens were connected, the stem portion of the precast section were placed on four supports. Each specimen was placed in position using the overhead crane in the Large-Scale Structures Lab at the Peter Kiewit Institute in University of Nebraska-Omaha campus and the grout for the shear key were cast while specimens are placed in testing configuration. Due to the stroke limitation with the hydraulic ram, a steel member and steel plates were placed between the hydraulic ram and the specimen. Load was applied at the

interface of the grouted shear key and the slab specimen as shown in Figure 4.13. The hydraulic loads were applied in a small increment during testing until there was a significant drop in load and the specimens were under rotation. Displacement was measured through string potentiometers placed next to the shear key in both sides at the location of loading point, quarter point, and at supports.

Figure 4.12: Full-Scale Specimen Test Setup

Figure 4.13: North-South and East-West view of the Test Setup

4.6 Test Results

4.6.1 Specimen F-M

Full-scale specimen with the mechanical joint (F-M) was tested first. Figure 4.14 is a close-up view of the grouted joint during testing. Similar to the behavior observed with small-scale specimens, the first crack initiated at the interface between the grout and the slab specimen.

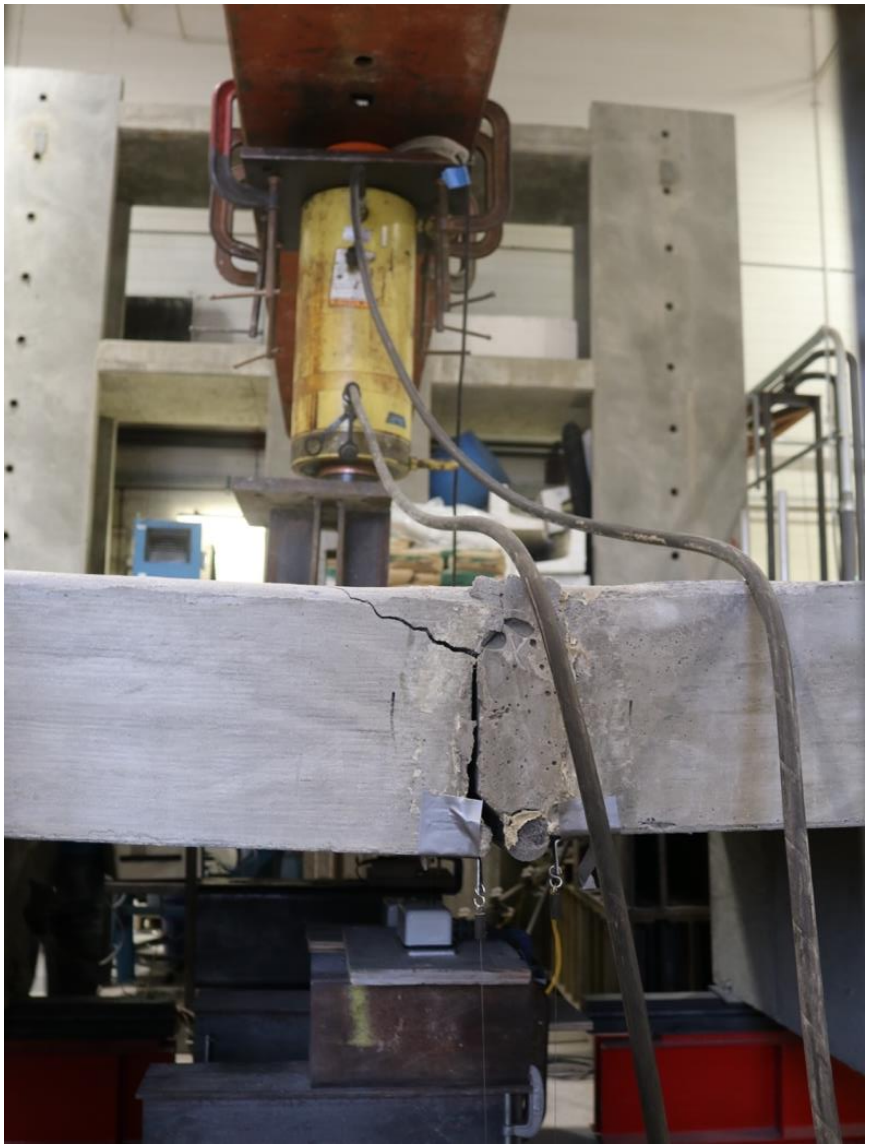

Figure 4.14: Close-up view of the Grouted Joint (Specimen F-M)

The test was terminated when the specimens were not able to take more load but started to rotate creating large deflections at the joint. Because no neoprene pads were supplied at the interface of the steel support and the slab specimens, inclined shear cracks were observed in the stem portion of the specimen near the supports and concrete cover started to spall off at that location as shown in Figure 4.15.

Figure 4.15: Specimen F-M at Failure

Figure 4.16 shows two photos taken from the bottom of the specimen. It is interesting to note that the shape of the crack close to the interface followed the angle of the Nelson-stud shear connectors on the mechanical joint which were placed in 45 degrees. After the completion of the testing, the two slab specimens were removed from the test setup, and as shown in Figure 4.17, the shape of the grout attached to the mechanical joint is the shape of the crack that was observed

underneath the slab specimen that is orientated based on the shape of the mechanical joint. It can be concluded that the failure mode was governed by insufficient length in development with the 8 in. Nelson studs in the joint system introduced in Figure 4.6.

Figure 4.16: Close-up view of the Grouted Joint (Specimen F-M)

Figure 4.17: Grout Shear Key Bond Failure (Specimen F-M)

The load-displacement curve for Specimen F-M is shown in Figure 4.17. The maximum load reached was 25.8 kip and the deflection at this load was 0.45 in. The tested joint moment would be 57 kip-ft (including the self-weight of the half of the flange) with the two mechanical connections in the 10 ft specimen. Each mechanical connection would carry approximately 28.5 kip-ft which are spaced at 4 ft spacing.

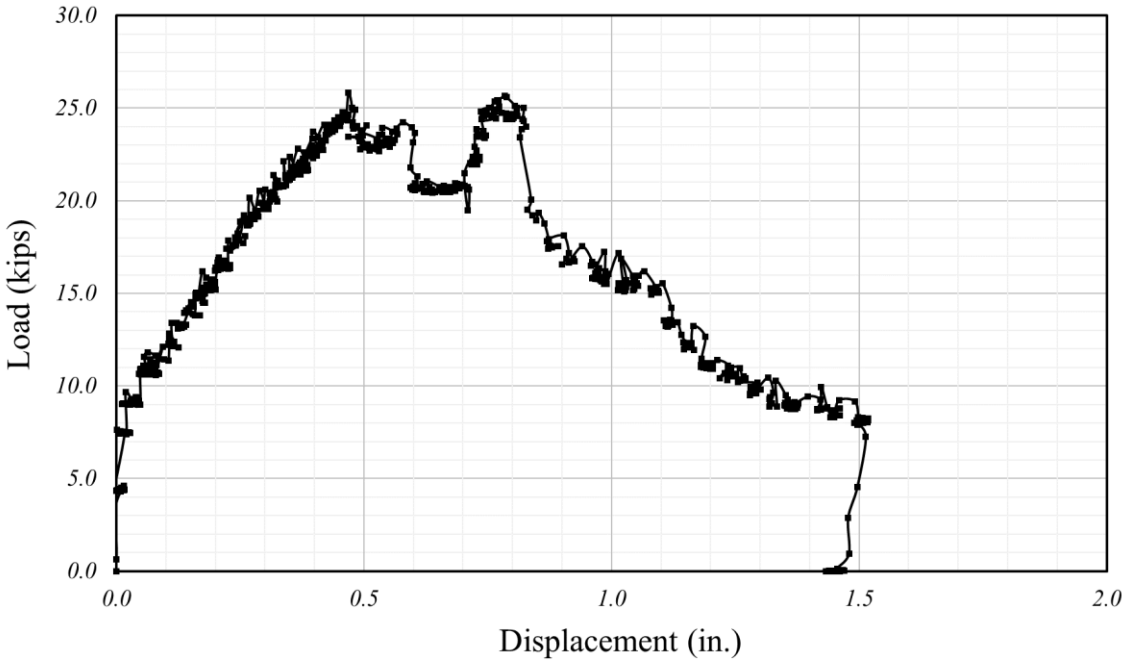

Figure 4.18: Load-Displacement of Specimen F-M

4.6.2 Specimen F-L-UHPC

The full-scale specimen with the staggered splice joint filled with a commercial ultra-high-performance concrete (Ductal - LafargeHolcim) joint was tested (F-L-UHPC). Figure 4.19 shows the test setup and loading in process. Figure 4.20 shows the load-displacement curve for Specimen F-L-UHPC.

Figure 4.19: Test Setup and Loading of Specimen F-L-UHPC

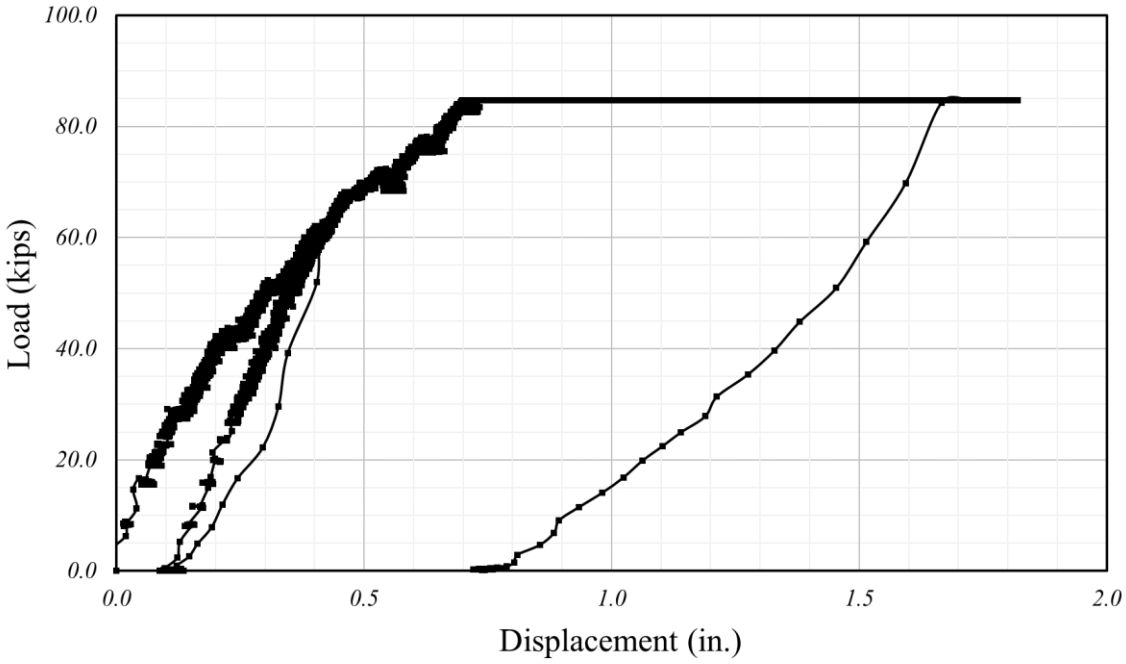

Figure 4.20: Load-Displacement of Specimen F-L-UHPC

With the ultra-high-performance concrete joint, the specimen was able to take 84.7 kips and the peak deflection was 0.72 in. After testing reached this maximum load the load did not increase and remained at the peak level while rotation was taking place. The test was terminated when cracks on the flange section were seen on the slab and inclined cracks were observed at the stem of the slab specimen. The tested joint moment would be 174.8 kip-ft (including the self-weight of the half of the flange) for the 10 ft specimen. This would be approximately 17.5 kip-ft per foot length. Comparing with the mechanical joint that was placed at 4 ft spacing, this would be more than two times the joint moment observed in the mechanical joint system.

4.6.3 Specimen F-R-SHPC

The full-scale specimen with the staggered splice joint filled with a Reno Super-High-Performance Concrete (F-R-SHPC) joint was tested using a mix that was being designed for the Nevada Department of Transportation. The main difference between the commercial UHPC and this new type of R-SHPC mix is that R-SHPC is a high strength, self-consolidating Fiber Reinforced Concrete (FRC) that would significantly reduce the cost and production limitations compared to UHPC and can be produced by a conventional drum-type mixer. The width of the joint was 6 in. as opposed to the 3 in. joint for the commercial UHPC. Figure 4.21 shows the test setup and loading in process. After the testing was complete, crack pattern was carefully observed by the research team. And as shown in Figure 4.22, the crack followed a pattern which would typically be observed in yield line analysis of two-way slab specimens. Inclined crack was formed stretching out between the load plate and the supports. Figure 4.23 shows the load-displacement curve for Specimen Reno-SHPC. With the Reno super-high-performance concrete, the specimen was able to reach comparable loads with F-L-UHPC (UHPC product commercially available) to 84.5 kips. After testing reached this maximum load, the load did not increase and

remained at the peak level while rotation was taking place as shown in Figure 4.23. Then, the load dropped during rotation and the test was terminated when cracks on the flange section were seen on the slab and inclined cracks were observed at the stem of the slab specimen. This was when the steel plates started to punch through the concrete resulting in punching shear failure mode. Comparing with the F-L-UHPC specimen (Figure 4.20), the initial stiffness was higher for F-R-SHPC specimen (Figure 4.23). This can be observed when comparing the displacement at specific load levels. For example, the displacement value at 40 kips and 60 kips are lower for F-R-SHPC compared to F-L-UHPC. However, the displacement at yield was both 0.7 in. at yield when load was approximately 85 kips for the two specimens. In addition, the load did not drop until we started to unload the specimen for F-L-UHPC specimen while there was a sudden drop in load while rotation was taking place for the F-R-SHPC specimen indicating that the commercial UHPC specimen had better ductility than the SHPC specimen.

Figure 4.21. Test Setup and Loading of Specimen F-R-SHPC

Figure 4.22. Crack Mapping and Failure of Specimen F-R-SHPC

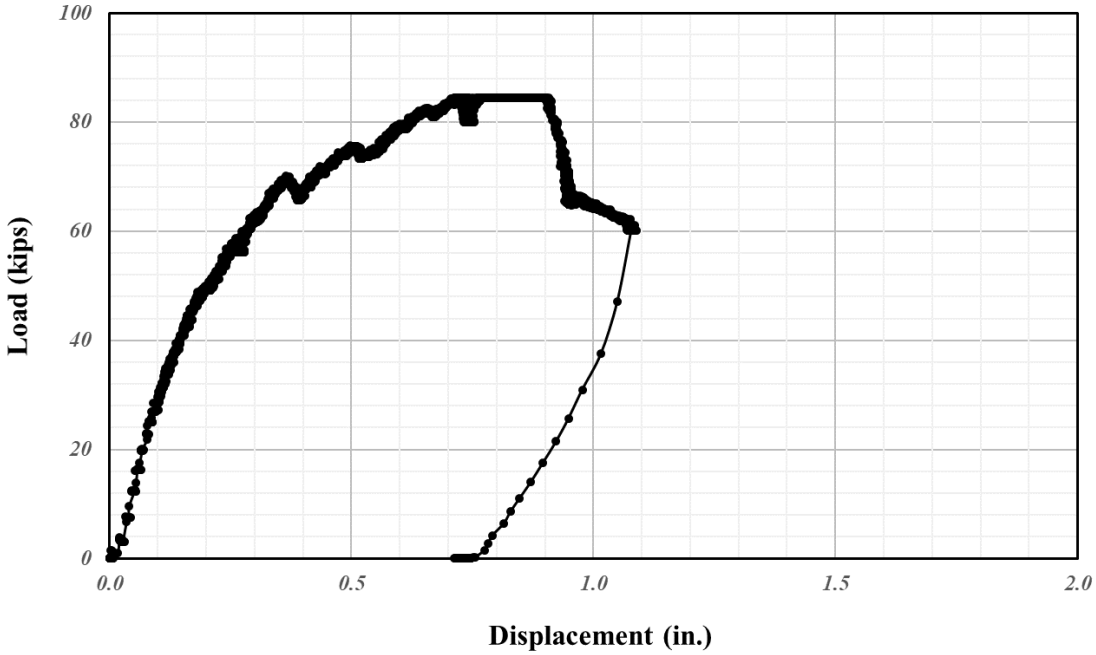

Figure 4.23. Load-Displacement of Specimen F-R-SHPC

4.6.4 Specimen F-N-SHPC

The full-scale specimen with the staggered splice joint filled with a Nebraska-Super-High-Performance Concrete (F-N-SHPC), a mix that was being designed for the Nebraska Department of Transportation was tested. This mix is also a high strength, self-consolidating Fiber Reinforced Concrete (FRC) that was developed with material available in Nebraska. Similar to R-SHPC, this mix can easily be produced by a conventional drum-type mixer and is cost effective compared to the commercial UHPC. For this test, a 6 in. joint was utilized due the No. 4 bars extruding outside the specimens 6 in. long. The lap was only 12 bar diameters with the 6 in. extension, but based on previous studies conducted by the FHWA's Turner-Fairbank Highway Research Center (Graybeal, 2014), this is sufficient lap slice length when high performance concrete is used. This was proved since the load-displacement curve generated through this flexural test was beyond yield capacity. Figure 4.24 shows the test setup and loading in process and Figure 4.25 shows the load-displacement curve.

Figure 4.24. Test Setup and Loading of Specimen F-N-SHPC

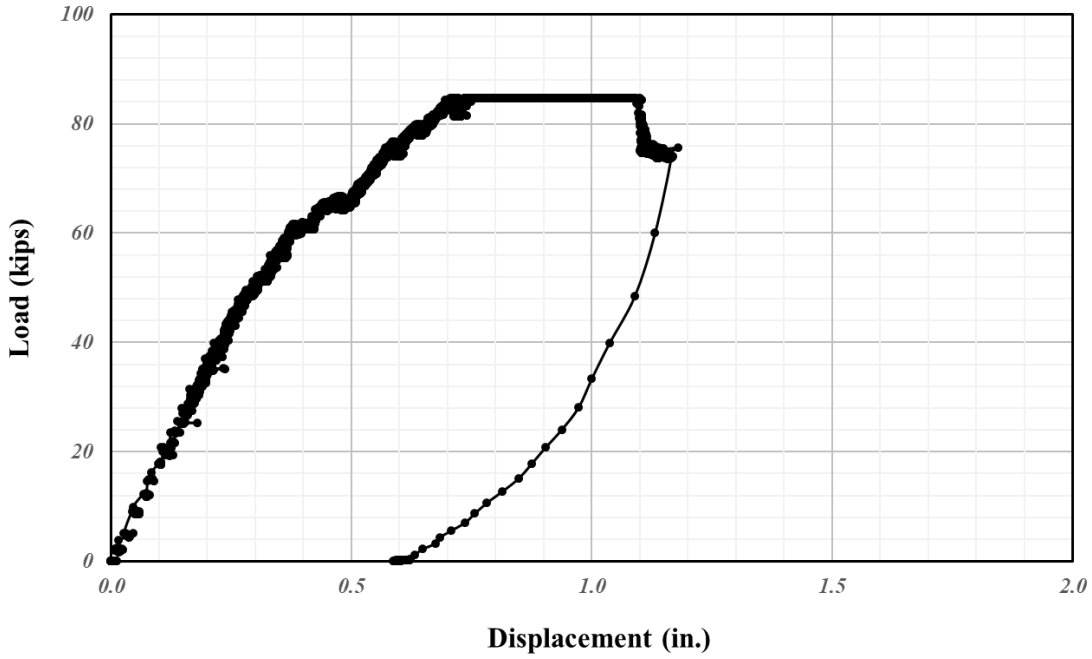

Figure 4.25. Load-Displacement of Specimen F-N-SHPC

With the Nebraska super-high-performance concrete, the specimen was able to reach up to 84.7 kips which is comparable load achieved by both the F-L-UHPC and F-R-SHPC specimen. Similar to the F-R-SHPC, the load was held while rotation was taking place and there was a sudden drop in load at 1.1 in. of deflection under the loading point. The test was terminated when load was not able to increase again. The initial stiffness for F-N-SHPC and the deflection at yield was similar to the F-L-UHPC. But, similar to the F-R-SHPC, this high strength self-consolidating fiber reinforced concrete specimen had less ductility than the F-L-UHPC which was able to rotate beyond a deflection of 1.5 in. at the location where loading was applied.

4.6.5 Specimen F-N-UHPC

The full-scale specimen with the staggered splice joint filled with an Ultra-High-Performance Concrete (UHPC) using a mix that was being designed for the Nebraska Department of Transportation (F-N-UHPC) was tested. Similar to other high-performance concrete specimens, the joint was 6 in. long due to the No. 4 reinforcement extending out of the proposed cross section with a lap slice length of 12 bar diameter. Figure 4.26 (a) shows the test setup and loading in process. Figure 4.26 (b) shows the punching shear failure mode observed at the top of the specimen where load was applied.

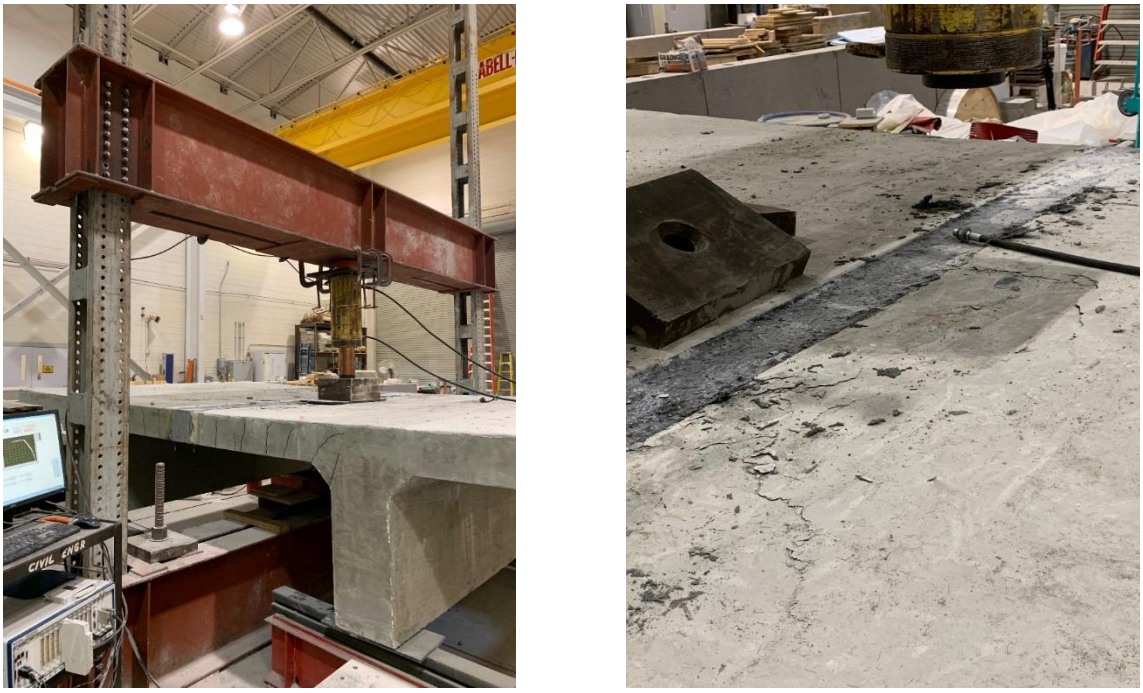

(a) Test setup (b) After failure

Figure 4.26. Test Setup and Loading of Specimen F-N-UHPC

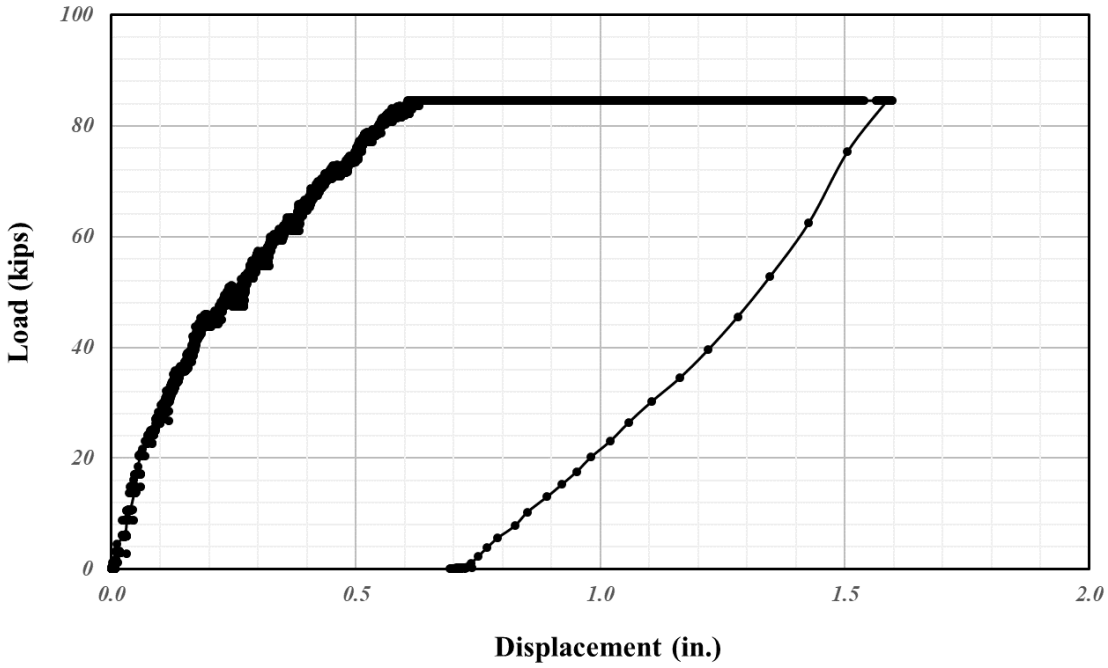

Figure 4.27. Load-Displacement of Specimen F-N-UHPC

The load-displacement curve for the F-N-UHPC specimen is shown in Figure 4.27. Similar to other specimens with super-high-performance or ultra-high-performance concrete, the yield load was 84.5 kips. Of special note, this specimen was able to rotate beyond a deflection of 1.5 in. where the load was applied. The testing was terminated due to the inclined cracks shown both on the bottom and the top of the specimen following the crack pattern typically estimated in yield line analysis of two-way slab systems. Unlike the F-R-SHPC or F-N-SHPC specimens, there was no drop in the load until the punching shear failure mode was observed demonstrating good ductility.

Figure 4.28 shows the load-displacement curve of all specimens with either super-high-performance concrete or ultra-high-performance concrete at the transverse joints. The initial stiffness varied between these four specimens with F-R-SHPC having the highest initial stiffness,

followed by the F-N-UHPC. The F-N-SHPC, and F-L-UHPC specimen had comparable initial stiffness. Although the initial stiffness of these specimens varied, they reached the yield strength of approximately 85 kips.

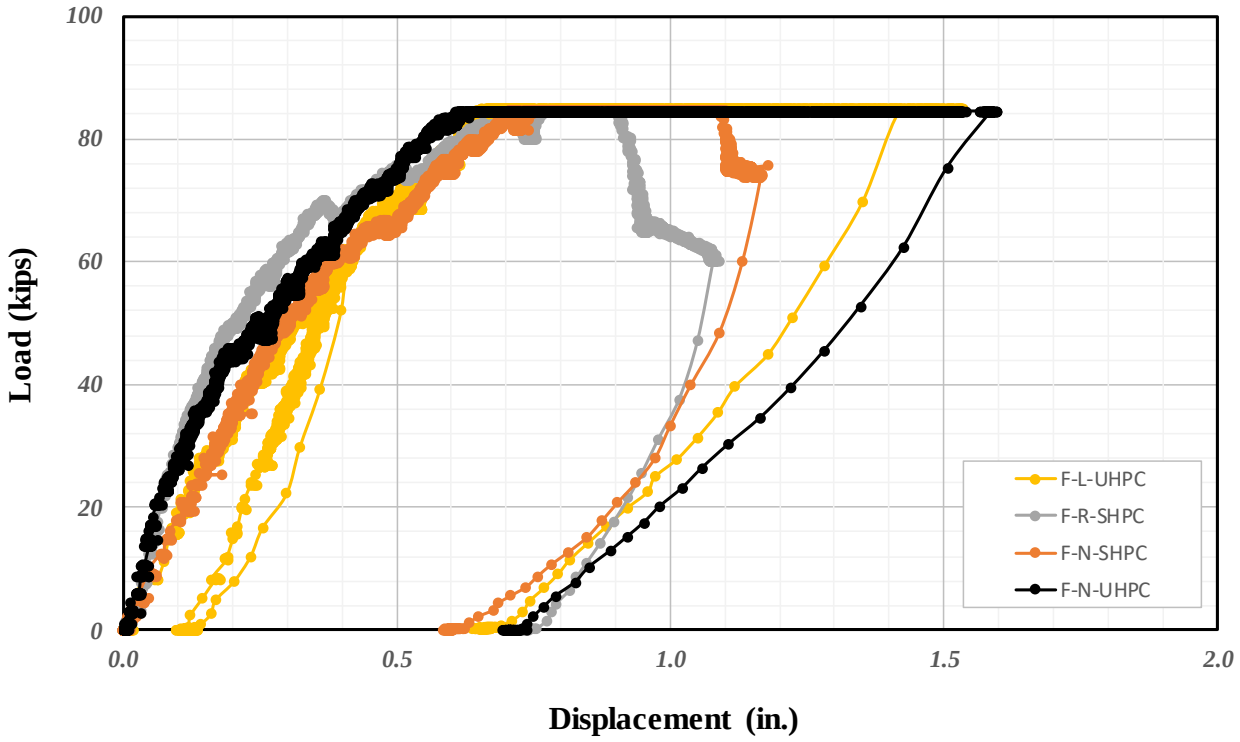

Figure 4.28. Load-Displacement of Specimens with Ultra-High-Performance or Super-High-Performance Concrete Joints

After the specimens reached the yield strength, the two T sections started to rotate with increase in deflection at the loading point without any damage observed at the transverse joint. The F-R-SHPC and the F-N-SHPC specimen that were high strength self-consolidating fiber reinforced concrete specimens developed for Nevada and Nebraska, respectively dropped in load capacity as it was pushed down. In comparison, the two UHPC specimens, one being the commercial mix (Ductal – LafargeHolcim) and the other being the mix developed at the University

of Nebraska-Lincoln, were loaded until punching shear failure was observed on the top and bottom of the top flange portion of the proposed T section. The transverse joints were still connecting the two T sections well and the entire system was behaving like two-way slab system under the point load at the joint. Both specimens behaved in a desirable behavior with good ductility until failure was reached.

4.7 Summary

Ten full-scale specimens that are 10 ft long were cast to evaluate the joint moment strength of various connections. This would include a mechanical joint, and several staggered splice joints with commercial ultra-high-performance concrete (Ductal - LafrageHolcim), and super-high-performance concrete or ultra-high-performance concrete designed by University of Nebraska with materials available in Nevada or Nebraska. Two proposed T section specimens were connected in transverse direction and tested. The joint moment carried per foot was 2.5 times larger when either the super-high-performance concrete or ultra-high-performance concrete was used as the grouting material in the shear key compared to the equivalent moment carried by mechanical joint system. None of the specimens with SHPC or UHPC joints failed prior to the T section failure.

CHAPTER 5. DESIGN RECOMMENDATIONS

5.1 Introduction

Based on the previous phase of research including an extensive literature review, small-scale testing, and full-scale testing, the research team have proposed a "flexible" precast cross section which is 8 ft wide and depending on the span length varies the depth between 1 to 3 ft. This cross section includes a 7.5 in. deck which reduces the cast-in-place construction and is wider than a typical single tee section. The proposed section has a wider web than typical single tee cross section but a shallower web than a typical bulb tee. The research team has conducted various small-scale testing with different transverse joint details including a new type of mechanical joint introduced in Chapter 3. The research team has also conducted full-scale testing with the mechanical joint system, staggered reinforcement with super-high-performance concrete or ultra-high-performance concrete. Test results and the proposed section was reviewed by the Technical Advisory Committee (TAC) members of the Nebraska Department of Transportation. Based on the discussion with the TAC members, the research team developed span charts of the proposed section and an equivalent solid plank section in this chapter. In addition, design charts for alternative plank sections with voids and different transverse connections than the current design is introduced in this chapter.

5.2 Span charts for the proposed sections

In this section, span charts for the proposed section and an 8 ft wide plank are produced for a concrete compressive strength of 5,000 psi and 8,000 psi. For both the proposed section and the 8 ft wide plank, span charts were developed for a cross section with a depth of 12 in., 18 in., or 24 in. as shown in Figure 5.1.

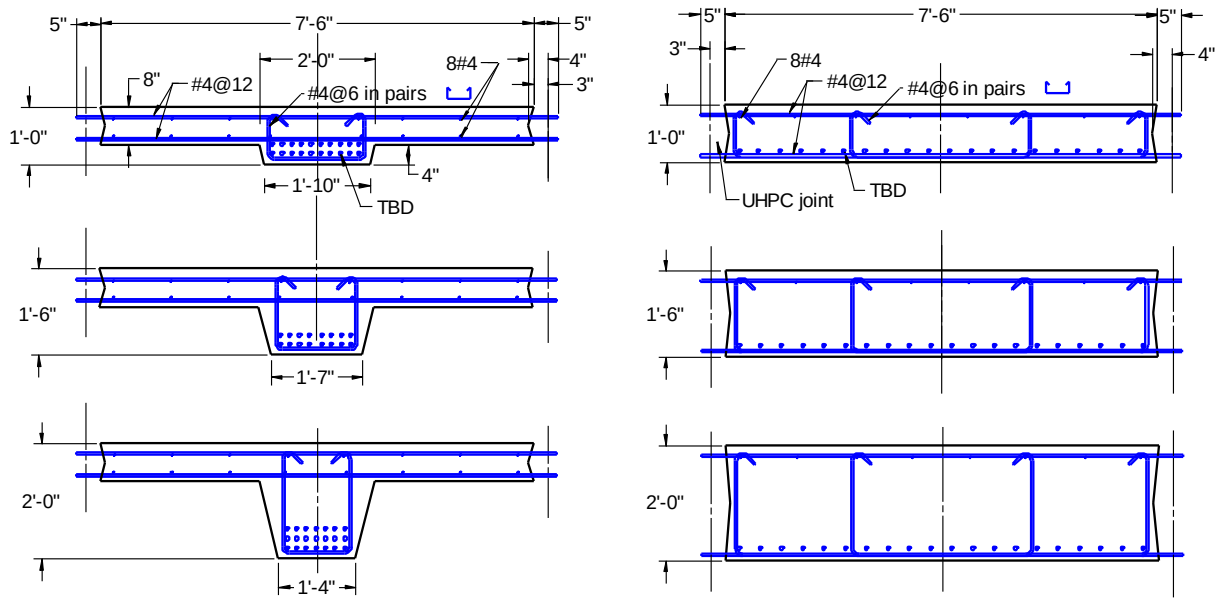

(a) Proposed standard cross section (b) Wide solid plank section

Figure 5.1. Proposed sections for span charts

Figures 5.2, 5.3, 5.4, and 5.5 show the design chart produced based on the parameters and assumptions made below. For all cases, ASTM A1035 high-strength reinforcement with a yield strength of 100 ksi were considered. The maximum reinforcement amount provided was based on having a tension controlled section ($\varepsilon_t = 0.005$) at ultimate to ensure a ductile design. A superimposed dead load of 37.5 psf (railing and wearing surface) and HL93 design live load were considered when producing these span charts. A live load distribution factor of S/11 (where S is the spacing of beams and units are in ft) was used in calculation. The span charts were generated with all these parameters including an assumption that there are no deflection limits.

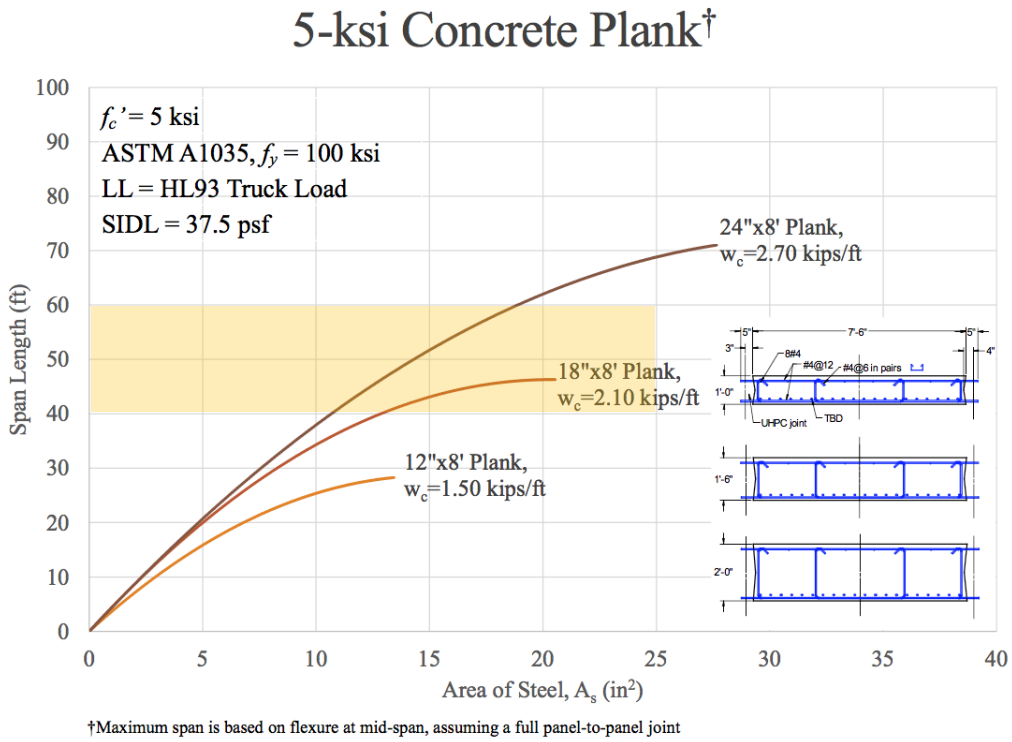

Figure 5.2. Design chart for wide concrete plank (f_c' =5,000 psi)

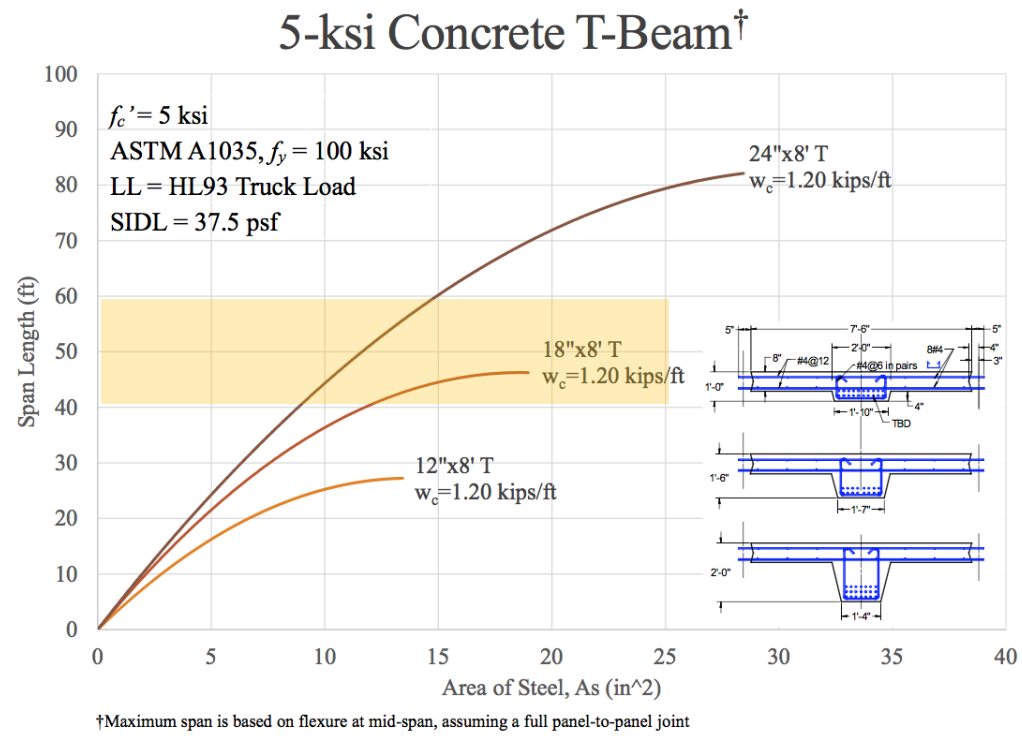

Figure 5.3. Design chart for proposed section (f_c' =5,000 psi)

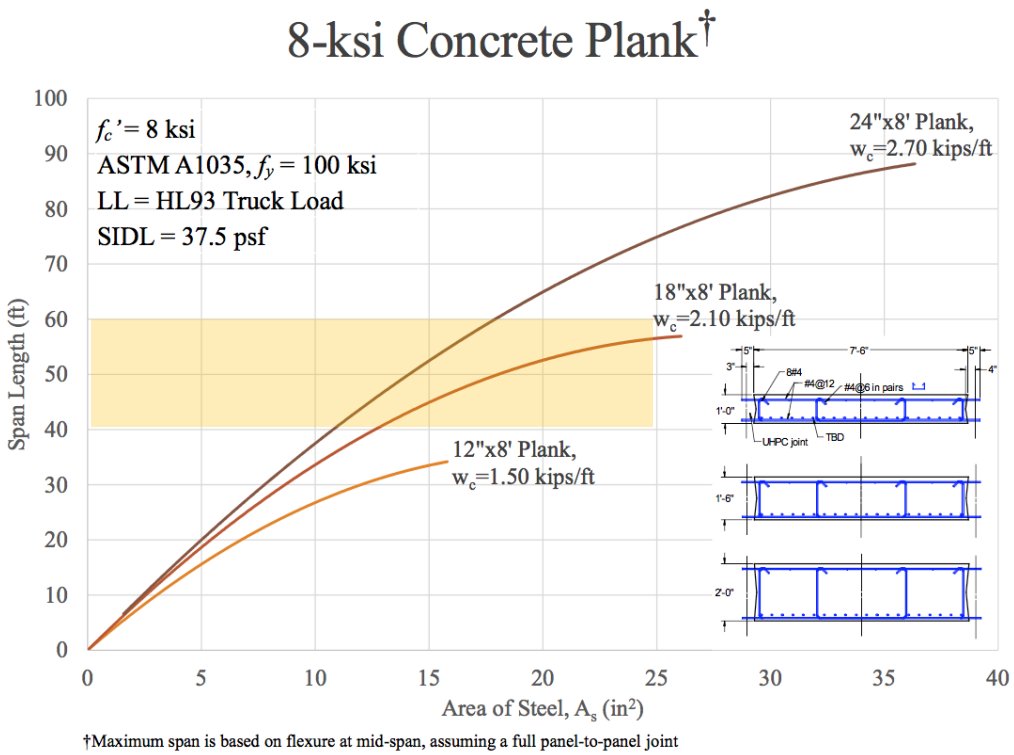

Figure 5.4. Design chart for wide concrete plank (f'_c =8,000 psi)

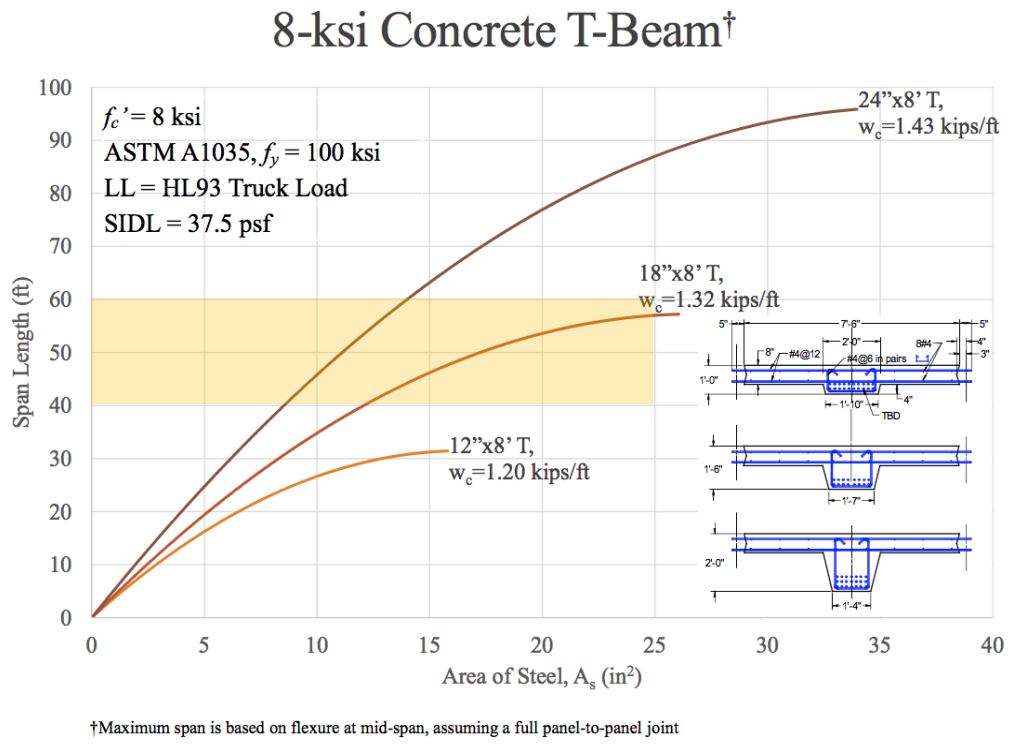

Figure 5.5. Design chart for proposed section (f'_c =8,000 psi)

The objective of this research was to provide a standard design for county bridges that can span up to 40 to 60 ft. This 40 to 60 ft span range is highlighted in Figure 5.2 to Figure 5.5. Although it may seem that the span chart is comparable for 8 ft by 12 in. section and the 8 ft by 18 in. section for concrete compressive strength of 5,000 psi (Figure 5.2 and 5.3), the difference becomes considerable for the 8 ft by 24 in. section. Specifically, when 15 or 20 square inch of reinforcement is used, the span length that can be achieved is different. A span length of 60 ft can be achieved with the 8 ft by 24 in. section with a concrete compressive strength of 5,000 psi when the total amount of reinforcement is 15 square in. This difference becomes clearer when 8,000 psi concrete is used and the span can be increased for the identical amount of steel used. Of special note, the weight difference is obvious between the wide plank section and the proposed section to span the equivalent length with the identical amount of steel. The 8 ft by 24 in. deep proposed section is only 44% in terms of weight compared to the 8 ft by 24 in. deep wide plank section. In addition, the 8 ft by 24 in. deep proposed section is lighter than the 8 ft by 12 in. solid plank section but can span approximately twice the length the 8 ft by 12 in. solid plank can span with the identical amount of steel provided.

5.3 Alternative plank and design charts

The proposed section is not very different than a wider plank with a stem in the middle which can easily be constructed as demonstrated in Chapter 4. However, in this section, other designs for using both solid and void planks without any stems are presented as an alternative option for contractors who prefer not to have stem cross sections. Figure 5.6 shows the cross section view of an alternative plank design. Figure 5.7 shows the top view of this suggested design.

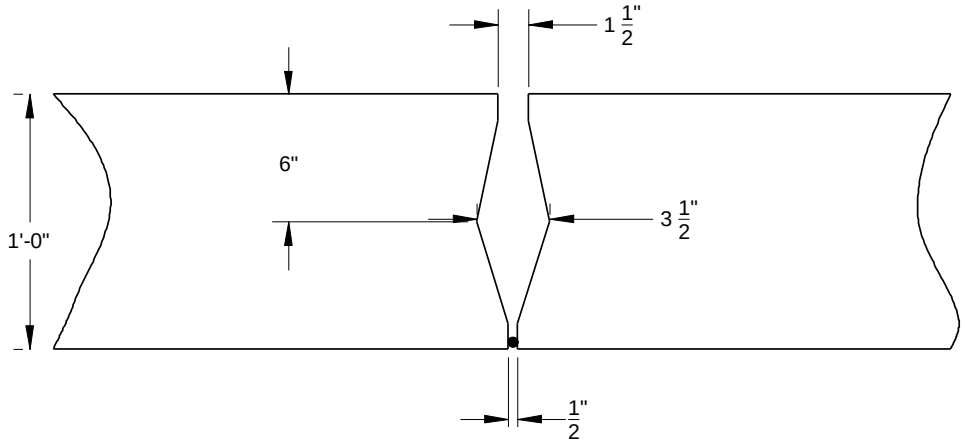

(a) Section between connections

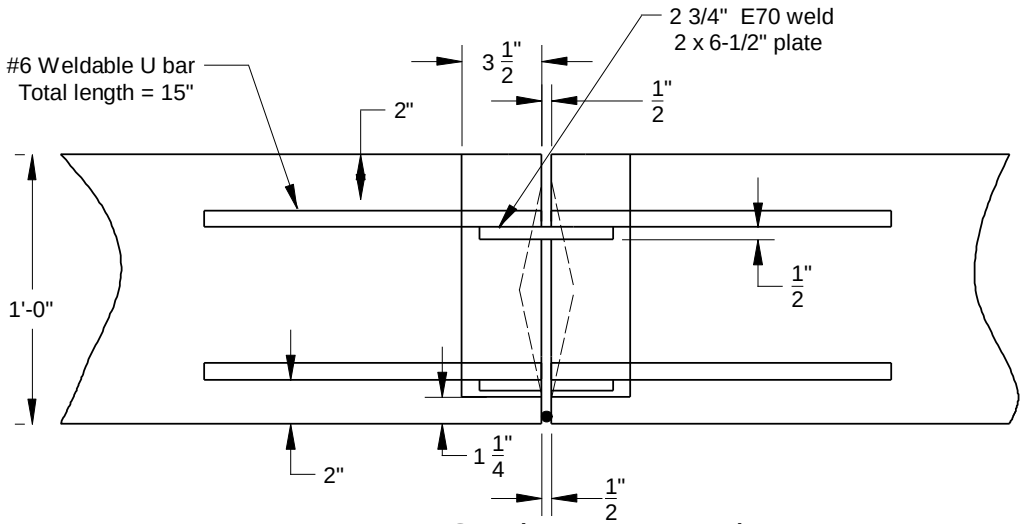

(b) Section at connections

Figure 5.6. Section view of the alternative plank design for Nebraska counties

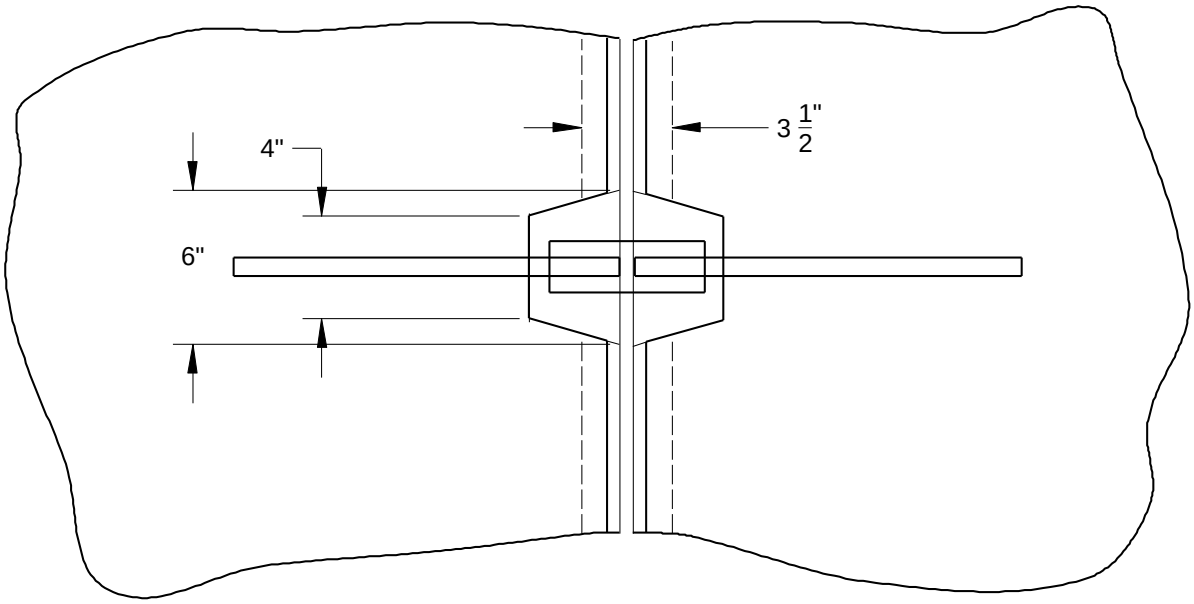

Figure 5.7. Top view of the alternative plank design for Nebraska counties

With the benefits of the developed ultra-high-performance concrete mix designs shown in Chapter 4, this joint detail can further be simplified by implementing these UHPC at the transverse joints of the planks and eliminate the welding plates and additional reinforcement required at the connections.

Regarding this alternative design, a design chart was produced for three different options. The first option contains a 4 ft wide and 12-in. thick alternative plank with the joint details introduced in Figure 5.6 and 5.7. The second option is considering a 4 ft wide and 12-in. thick solid plank but with UHPC used for both the plank section and the joint. The third option is a 4 ft wide and 18-in. thick voided plank (hollow section suggested to reduce the weight) and UHPC used for both the cross section and the joint. The joints for UHPC solid and voided plank is assumed to be filled with UHPC and 1.5 in. wide at the mid-height of the joint. The planks in the first option constructed with conventional concrete is assumed to have a concrete

compressive strength of 5,000 psi and Grade 60 steel. The solid and voided plank for the second and third option is assumed to have a concrete compressive strength of 18,000 psi and ASTM A1035 steel with Grade 100 steel. For these alternative planks, prestressing is additionally considered as an option with target f_{ps} of 250 ksi. To satisfy the deflection limits, the span-to-depth ratio is assumed not to exceed 30. HL93 design live load is applied and the edge-to-edge bridge with is assumed to be 28 ft and 9 in with two design lanes. The wearing surface is assumed to be 35 pounds per square foot. With the parameters chosen above, the span charts for the alternative planks for the three options are shown in Figure 5.8.

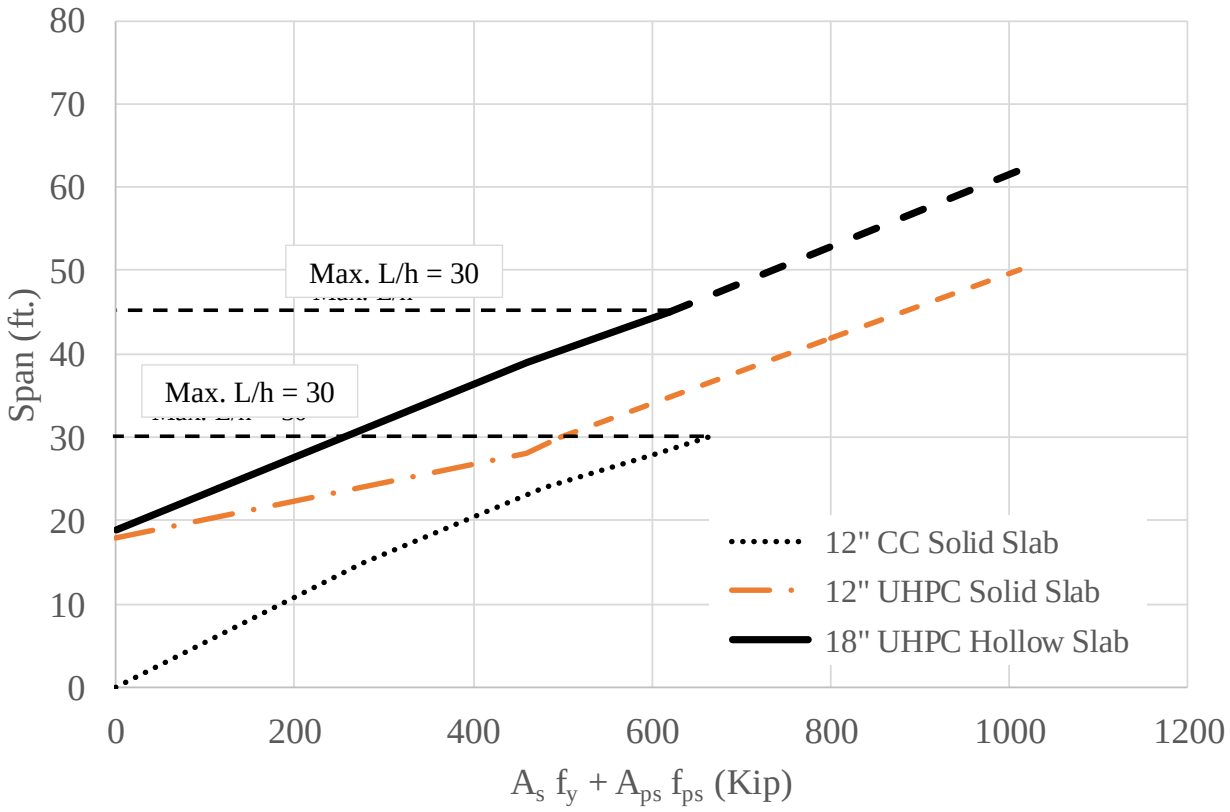

Figure 5.8. Design chart for alternative planks

5.4 Summary

In this chapter, span charts of the proposed section (Single T section with various depth) and wide solid plank (8 ft wide) were provided. In addition, span charts for alternative plank designs with either a solid or voided planks were provided. Nebraska counties may select the design that will suit best for their needs for replacing aging county bridges. However, the proposed 8 ft wide single T section with 2 ft depth will provide the best economical and structural solution for the needs. The current welded joints can be replaced with either the new type of mechanical joint or UHPC or SHPC (mix designs developed at UNL) joints to improve both the strength and serviceability concerns.

CHAPTER 6. SUMMARY AND CONCLUSIONS

6.1 Overview of Research

Many of the Nebraska county bridges need replacement due to their structural deficiency. Most of the bridges needing replacement are in the 40 to 60 ft range. This span range appears to be lacking a standard design that fits Nebraska county practices in terms of speed and simplicity of construction. The current system being used are (a) Precast 1 by 2 ft planks which can span up to 30 ft, (b) Cast-in-place slab bridges which can span up to 50 ft but require extensive field formwork, concrete placing, and curing, and are best when constructed in three-span units, and (c) Inverted tees which can span 40 to 80 ft, but require cast-in-place decks.

The objective of this research project is to develop and evaluate a cross section that can be modified to be used for spans up to 40 to 60 feet, while reducing the number of longitudinal shear keys, and retaining the ease of construction by the plank design. Four phases of research were conducted to achieve this objective. The first phase included evaluating various sections for spans up to 60 ft. This was completed through an extensive literature review and a new type of cross-section was proposed in this study. The second phase of the research included evaluating a new type of transverse connection that could possibly be used for the proposed state county bridge system through small-scale testing on ten slab specimens. The third phase of the research tested five-sets of full-scale bridge specimens to evaluate the behavior of transverse connection that includes the new type of mechanical connection, staggered splice joint with commercial ultra-high-performance concrete, super-high-performance concrete developed for Nevada and Nebraska, and ultra-high-performance-concrete developed at UNL used for the shear key.

Based on the literature review that includes computational analysis, experimental testing, field monitoring, and synthesis studies on bridges with adjacent beams it was clear that the lateral load distribution and load transfer between individual beams are highly dependent on the keyway joint details. Although, many different types of shear keyways were developed from the nationwide surveys and field measurements, it was identified that these grouted joints still crack, create longitudinal cracks on top of the bridge deck, and create a path for water or chloride leakage. Many state and county engineers and precast producers identified that the solutions to this recurring problem could be 1) providing a full-depth shear key, 2) post-tensioning the adjacent beams in transverse direction, or 3) topping these adjacent beams with cast-in-place deck.

In order to resolve the problems seen in this literature survey without complicating the construction for counties (not introducing post-tensioning, or including cast-in-place decks), this study suggested a precast single tee cross section (wider than typical tee sections with wider web) that could be constructed with a single formwork that works for variable depth.

6.2 Experimental Program

6.2.1 Mechanical Connection Test Program

The objective of this phase of the research is to investigate the shear and moment capacity of a new type of mechanical connection that is proposed to be used in connecting adjacent precast bridge sections proposed in this study. Each mechanical joint consists of four all threads with nuts, an alignment plate, an anchor plate, and a 1.25 in. ASTM A490 bolt with nut to connect the two slabs. Three and four-point bending tests were conducted to evaluate the joint shear and moment of the proposed mechanical connection for adjacent bridge sections.

Ten slabs were casted to evaluate the joint capacity of five connected slab specimens. Threaded bars with fine threads, coarse threads, and a mix of each of them were tested. The threaded bars with fine threads had the best performance. It was noted that although the joint did not carry more moment after exceeding the capacity, it did allow additional rotation to take place. On average, the experimental joint moment was 38 ft-kip and the tested joint shear was 17 kip.

6.2.2 Full-Scale Test Program

The objective of this phase of research is to investigate the shear and moment capacity of the new type of mechanical connection that was tested in small-scale as a proof of concept, in full-scale with the cross sections that would be used in the field. For this testing program, the 8 ft wide, 2 ft deep cross section which can span up to 50 ft was divided into five 10 ft long specimens. Five sets of these specimens were cast (ten specimens in total). The 10 ft long sections were connected through the mechanical connection proposed in small-scale test program. In addition to the mechanical joint, a staggered rebar splice joint grouted with a commercial mix of ultra-high-performance concrete, a super-high-performance-concrete (high strength self-consolidating fiber reinforced concrete) mix design developed with material available in Nebraska and Nevada, and ultra-high-performance concrete developed in University of Nebraska-Lincoln to evaluate different systems. Test results indicated that the joints grouted with either the ultra-high-performance concrete or super-high-performance concrete carried a joint moment of 17.5 kip-ft per foot length which is 2.5 times larger than the equivalent moment carried by the mechanical joint system with non-shrink grouts.

BIBLIOGRAPHY

AASHTO (1957), *Standard Specifications of Highway Bridges*, 7th Edition, American Association of State Highway and Transportation Officials, Washington, D.C., 22 pp.

AASHTO (2010), *AASHTO LRFD Bridge Design Specifications*, American Association of State Highway and Transportation Officials, Washington, D.C., 1591 pp.

American Society for Testing and Materials (ASTM). (2018), "Standard Test Method for Compressive Strength of Cylindrical Concrete Specimens." C 39-18, West Conshohocken, Pa.

American Society for Testing and Materials (ASTM). (2017), "Standard Test Method for Splitting Tensile Strength of Cylindrical Concrete Specimens." C 496-17, West Conshohocken, Pa.

American Society for Testing and Materials (ASTM). (2016), "Standard Test Method for Compressive Strength of Hydraulic Cement Mortars (Using 2-in. or [50-mm] Cube Specimens)." C 109-16a, West Conshohocken, Pa.

El-Remaily, A., Tadros, M.K., Yamane, T., and Krause, G. (1996), "Transverse Design of Adjacent Precast Prestressed Concrete Box Girder Bridges," *PCI Journal*, Vol. 41, No. 4, pp. 96–113.

Graybeal, B. (2014), "Bond Behavior of Reinforcing Steel in Ultra-High-Performance Concrete," FHWA-HRT-14-089 Technical Report, McLean, VA, 12 pp., http://www.fhwa. dot.gov/publications/research/infrastructure/structures/ bridge/14090/index.cfm.

Greuel, A., Baseheart, T.M., Rogers B.T., Miller, R.A., and Shahrooz, B.M. (2000), "Evaluation of a High Performance Concrete Box Girder Bridge," *PCI Journal*, Vol. 45, No. 6, pp. 60–71.

Hanna, K.E., Morcous, G., Tadros, M.K. (2009), "Transverse Post-Tensioning Design and Detailing of Precast Prestressed Concrete Adjacent Box Girder Bridges," *PCI Journal*, Vol. 54, No. 4, pp. 160–174.

Hanna, K., Morcous, G., Tadros, M.K. (2011), "Adjacent Box Girders without Internal Diaphragms or Post-tensioned Joints," *PCI Journal*, Vol. 56, No. 4, pp. 51–64.

Huckelbridge, A.A., El-Esnawi, H., and Moses, F. (1995), "Shear Key Performance in Multibeam Box Girder Bridges," *Journal of Performance of Constructed Facilities*, Vol. 9, No. 4, pp.271-285.

Jones, H. L. (1999), "Multi-Box Beam Bridges with Composite Deck," FHWA/TX-00/1709-1, Texas Transportation Institute, Texas A&M University, College Station, TX, 123 pp.

Jones, H. L. (2001), "Lateral Connections for Double Tee Bridges," FHWA/TX-01/1856-2, Texas Transportation Institute, Texas A&M University, College Station, TX, 101 pp.

Lall, J., Alampalli, S., and Dicocoo, E.F. (1998), "Performance of Full-Depth Shear Keys in Adjacent Prestressed Box Beam Bridges," *PCI Journal*, Vol. 43, No. 2, pp. 72–79.

Miller, R. A., Hlavacs, G.M., and Long, T.W. (1998), "Testing of Full Scale Prestressed Beams to Evaluate Shear Key Performance," FHWA/OH-98/019, Federal Highway Administration, Washington, D.C., 96 pp.

Naito, C.J., Sause, R., Hodgson, I., Pessiki, S., and Macioce, T. (2010), "Forensic Examination of a Noncomposite Adjacent Precast Prestressed Concrete Box Beam Bridge," *ASCE Journal of Bridge Engineering*, Vol. 15, No. 4, pp.408-418.

Newmark, N.M., and Siess, C.P. (1942), "Moments in I-Beam Bridges," Engineering Experiment Station Bulletin No. 336, College of Engineering, University of Illinois, Urbana, IL, 149 pp.

Pool, R.B., Arya A.S., Robinson, A.R., and N. Khachaturian, N. (1965), "Analysis of Multibeam Bridges with Beam Elements of Slab and Box Section," Engineering Experiment Station Bulletin No. 483, Vol. 62, No. 106 (July), College of Engineering, University of Illinois, Urbana, IL, 33 pp.

Russell, H.G. (2009), "Adjacent Precast Concrete Box-Beam Bridges: Connection Details," National Cooperative Highway Research Program (NCHRP) Synthesis 393, Transportation Research Board, National Research Council, Washington, D.C., 83 pp.

Russell, H.G. (2011), "Adjacent Precast Concrete Box-Beam Bridges: State of the Practice," *PCI Journal*, Vol. 56, No. 1, pp. 75–91.

Stanton, J. F., and Mattock, A.H. (1986), "Load Distribution and Connection Design for Precast Stemmed Multi-Beam Bridge Superstructures," NCHRP Report 287, Transportation Research Board, National Research Council, Washington, D.C., 137 pp.